

Large Scale Structure at $z = 1.2$ Outlined by MgII Absorbers⁰

Gerard M. Williger^{1,2,3}

williger@pha.jhu.edu

Luis E. Campusano⁴

luis@das.uchile.cl

Roger G. Clowes⁵

rgclowes@uclan.ac.uk

Matthew J. Graham⁶

m.j.graham@ic.ac.uk

ABSTRACT

The largest known structure in the high redshift universe is mapped by at least 18 quasars and spans $\sim 5^\circ \times 2.5^\circ$ on the sky, with a quasar spatial overdensity of 6–10 times above the mean. This large quasar group provides an extraordinary laboratory $\sim 100 \times 200 \times 200h^{-3}$ comoving Mpc^3 in size ($q_0 = 0.5$, $\Lambda = 0$, $H_0 = 100h \text{ km s}^{-1} \text{ Mpc}^{-1}$) covering $1.20 < z < 1.39$ in redshift. One approach to establish how large quasar groups relate to mass (galaxy) enhancements is to

⁰Based on observations with the Blanco 4m telescope at CTIO, which is operated by the Association of Universities for Research in Astronomy, Inc. under contract to the National Science Foundation.

¹Laboratory for Astronomy and Solar Physics, NASA Goddard Space Flight Center, Code 681, Greenbelt MD 20771, USA

²National Optical Astronomy Observatory, P.O. Box 26732, Tucson AZ 85716–6732

³present address: Dept. of Physics & Astronomy, Johns Hopkins University, Baltimore MD 21218, USA

⁴Departamento de Astronomía, Universidad de Chile, Casilla 36-D, Santiago, Chile

⁵Centre for Astrophysics, University of Central Lancashire, Preston PR1 2HE, UK

⁶Blackett Laboratory, Imperial College, London SW7 2BW, UK

probe their gas content and distribution via background quasars. We performed a survey for Mg II absorption systems in a $\sim 2.5^\circ \times 2.5^\circ$ subfield in the large quasar group, and found 38 absorbers to a rest equivalent width limit of $W_0 = 0.3 \text{ \AA}$ over $0.69 < z < 2.02$. Only 24 absorbers were expected, thus we find a 2σ overdensity over all redshifts in our survey. We have found the large quasar group to be associated with 11 Mg II absorption systems at $1.2 < z < 1.4$; 0.02%–2.05% of simulations with random Mg II redshifts match or exceed this number in that redshift interval, depending on the normalization method used. The minimal spanning tree test also supports the existence of a structure of Mg II absorbers coincident with the large quasar group, and additionally indicates a foreground structure populated by Mg II absorbers and quasars at $z \sim 0.8$. Finally, we find a tendency for Mg II absorbers over all redshifts in our survey to correlate with field quasars (i.e. quasars both inside and outside of the large quasar group) at a projected scale length on the sky of $9h^{-1}$ Mpc and a velocity difference $|\Delta v| = 3000$ to 4500 km s^{-1} . While the correlation is on a scale consistent with observed galaxy-AGN distributions, the nonzero velocity offset could be due to the “periphery effect”, in which quasars tend to populate the outskirts of clusters of galaxies and metal absorption systems, or to peculiar velocity effects.

Subject headings: cosmology: observations – galaxies: quasars: absorption lines
– galaxies: intergalactic medium

1. Introduction

Evidence is mounting for the existence of super large scale structure on the scale of several tens of Mpc. At low redshift ($v \lesssim 40,000 \text{ km s}^{-1}$), galaxy surveys reveal structures exceeding $\sim 50h^{-1}$ Mpc in size (e.g. Geller et al. 1997; Doroshkevich et al. 2000, and references therein), and there are indications for deviations from homogeneity out to scales of $160 h^{-1}$ Mpc (Best 2000). Structures of comparable size have been noted in simulations of cosmological evolution, e.g. patterns of wall-like structure elements with diameter $\sim 30 - 50h^{-1}$ Mpc which surround low density regions with typical largest extension $\sim 50 - 70h^{-1}$ Mpc (Demianski & Doroshkevich 2000). Such super large scale structure may be understood in the context of the Zel’dovich nonlinear theory of gravitational instability (Doroshkevich et al. 1999, and references therein). Large-box simulations can reproduce the main properties of the observed large scale matter distribution, including structures having a clumpy wall-like morphology, and which incorporate $\sim 50\%$ of matter with an overdensity of $\sim 5 - 10$ above the mean. Super large scale structure thus should provide a potentially efficient way

to study large numbers of galaxies in a similar environment, their distribution and how they relate to phenomena such as quasars.

The most stringent constraints on models which predict the existence of very large scale structures should be provided by measuring their properties at early times in their evolution and thus at the highest possible redshifts. However, at redshifts higher than a few tenths, which is the regime accessible from large galaxy surveys, probing the observational characteristics of super large scale structure becomes a challenge. One way to observe super large scale structure beyond the distances offered by large galaxy surveys is to use brighter test objects, viz. quasars, which are much more easily detected than galaxies at $z > 1$. An additional advantage for tracing large structures offered by quasars is their intrinsic low volume density compared to galaxies, so that a small number of them can be used to delineate structures over regions where the expected number is on the order unity (tens of Mpc). The low intrinsic space density and large luminosities of quasars have already been exploited to this end: structures outlined by them spanning from tens to hundreds of Mpc have been discovered at $z > 1$. These large quasar groups (e.g. Webster 1982; Crampton, Cowley, & Hartwick 1987, 1989; Clowes & Campusano 1991; Graham, Clowes, & Campusano 1995; Clowes, Campusano, & Graham 1999; Clowes 2001, ~ 20 are known to date) may represent high redshift precursors of large wall-like structures (e.g. Komberg & Lukash 1994). Large quasar groups are not only ideal laboratories for studying the physical characteristics of large density perturbations in the universe, but also for the inter-relation between the quasars, galaxies and gas contained within. One difficulty is that quasars themselves trace the highest overdensity mass perturbations, and thus are expected to be the most highly biased tracers of mass and to cluster the most strongly, cf. Silk & Weinberg (1991). Therefore, quasars in large quasar groups do not by themselves reveal much about the distribution of more common, lower mass objects in the same region. However, if the mass bias as a function of redshift for the quasars in large quasar groups could be determined, then they would provide an efficient means to map out the large scale distribution of matter at high redshift.

The relative overdensity of various forms of matter (galaxies, gas) in large quasar groups (or in super large scale structure) is not well determined. From simulations, Doroshkevich et al. (1999) found that from the present epoch to $z \sim 1$, the fraction of matter accumulated by the largest wall-like structures for a given density drops by a factor of ~ 2 and becomes negligible by $z = 3$. They suggested that detailed statistical descriptions of quasar absorbers are required to probe the characteristics of super large scale structures at such epochs. The advantage of quasar absorbers is that they trace much lower mass overdensities than quasars themselves, and thus offer a much more detailed picture of the overall mass distribution.

We have used Mg II absorbers for just such a study, as a high redshift pencil-beam

complement to low redshift galaxy surveys. Quasar metal absorbers delineate large structures up to $100 h^{-1}$ Mpc (Quashnock et al. 1996; Quashnock & Stein 1999). Mg II absorbers with rest equivalent width $W_{0, MgII\ 2796} \geq 0.3 \text{ \AA}$ have been strongly linked to galaxies out to $z \sim 1.2$ (e.g. Steidel et al. 1997; Guillemin & Bergeron 1997), and thus provide a gas cross-section selected galaxy sample, highlighting the cosmic web of filaments and sheets which appear to constitute large scale structure (e.g. Cen & Simcoe 1997).

An optimal region to use for a quasar–Mg II overdensity comparison is the largest structure known at $z > 1$. It consists of a large quasar group of at least 18 and possibly 23 quasars at $1.20 < z < 1.39$ toward ESO/SERC field 927 (Clowes & Campusano 1991; Clowes, Campusano, & Graham 1995, 1999; Newman et al. 1998), which spans $\sim 5^\circ \times 2.5^\circ$ on the sky, and has a bright quasar space density in the region ~ 6 – 10 times greater than average. It is ideal for study due to its large size and relative proximity, thus allowing the observation of $z \sim 1.3$ associated galaxies over a range of luminosities. From deep optical/IR images in a subfield of the large quasar group, there is evidence of a galaxy cluster merger and a general excess of red galaxies around the $z \approx 1.23$ quasar J104656+0541 to a surrounding radius of 0.25° , which are probably associated with the large quasar group (Haines 2001; Haines et al. 2001). We have taken spectra of 23 quasars within and behind the large quasar group, to make a survey for Mg II absorbers in the region. In the following sections, we describe the spectra, sample selection, statistical tests to detect overdensities and structures around the large quasar group as defined by the Mg II absorbers and our interpretations of the results.

2. Observations

We obtained spectra for 23 quasars ($1.23 < z_Q < 2.68$) in a $2.5^\circ \times 2.5^\circ$ field toward the Clowes & Campusano large quasar group with the CTIO-4m Blanco telescope and RC spectrograph (grating 181, Loral 3k \times 1k CCD, $1.99 \text{ \AA}/\text{pixel}$, $\sim 6.7 \text{ \AA}$ resolution). Observations were on the nights of 1997 March 30, April 1 and 1999 March 30, 31. The useful wavelength coverage was 4600–9250 \AA ($0.64 < z < 2.30$ for MgII $\lambda\lambda 2796, 2804$). Conditions were photometric with 1.1–1.8 arcsec seeing. There were between one and seven exposures per object, with total exposure times ranging from 900 to 10696 seconds.

The basic spectral reductions were performed with IRAF, and the spectra were summed using inverse variance weighting with cosmic ray rejection routines in IDL, provided by R. Hill of the Space Telescope Imaging Spectrograph group at NASA Goddard Space Flight Center. A 1σ error array was propagated throughout the reductions for each spectrum, and confirmed with measurements of the variation about the mean in selected parts of the spectra. The wavelengths were corrected to vacuum heliocentric values. Quasar positions,

redshifts (based on the lowest ionization lines available in the spectra), and photometry (Keable 1987; Clowes & Campusano 1994; Clowes, Campusano, & Graham 1999) are given in Table 1.

3. Selection of samples

For statistical analysis, we selected two samples of Mg II absorbers based on the rest equivalent width of the $\lambda 2796$ Å line. In addition, we chose a sample of quasars from our work and the literature, to test for correlations between Mg II absorbers and quasars. Finally, we note the existence of other metal transitions, possible damped Ly α systems and the properties of a peculiar quasar in our sample.

3.1. Selection of Mg II sample

To make a sample of Mg II absorption systems, we first created a continuum for each summed spectrum with standard IRAF packages. Next, regions of contiguous pixels were selected for each spectrum in which the flux was below the continuum. The equivalent width and corresponding error for each region were calculated to create a list of features at $\geq 5.0\sigma$ significance. We provide wavelengths of all features at $\geq 5.0\sigma$ significance for reference to future higher resolution studies, to verify the existence of any metals identified in future based on higher resolution spectra or additional data from the Ly α forest.

In addition, for the sole purpose of identifying components of Mg II doublets and other metal lines associated with them, a secondary line list of features at $> 2.5\sigma$ significance was created. The wavelengths of the absorption features were examined for pairs consistent with the Mg II $\lambda\lambda 2796, 2803$ doublet ratio, with the requirement that the stronger $\lambda 2796$ line be significant at $\geq 3\sigma$.

The spectral resolution of 6.7 Å is sufficient to resolve the Mg II doublet, but not to resolve blended complexes. Therefore, as a check, each of the authors examined each spectrum by eye, using velocity plots of the Mg II $\lambda\lambda 2796, 2803$, to confirm the reality of each Mg II system. As a further quality control measure for the doublet wavelength ratio constraint, a majority (75%) vote of the authors was required to deem a Mg II system as real. We find a total initial sample of 41 “real” Mg II systems (plus five candidates and one less likely one classified as “doubtful”), with the least significant “real” Mg II system possessing $\sigma_{\lambda 2796} = 3.36$, $\sigma_{\lambda 2803} = 2.66$ (4.3σ summed in quadrature). Plots of each quasar spectrum are in Fig. 1. We have indicated zones in which line profiles may be blended with telluric

absorption, determined by 1) normalizing each quasar spectrum, taking a median of the ensemble of normalized individual quasar spectra and searching for features common to all spectra, and 2) visually inspecting each spectrum to look for regions of absorption which are common to most or all objects. Expanded plots of the Mg II doublets in velocity space are in Fig. 2. A list of features significant at $\geq 5.0\sigma$, plus a small number of identified Mg II components and other metals at $< 5\sigma$ significance associated with Mg II absorbers, is in Table 2.

To compare our Mg II absorber sample with one from the literature, we define “strong” and “weak” samples with rest equivalent width thresholds of 0.6 and 0.3 Å, respectively, for the Mg II $\lambda 2796$ line (Steidel & Sargent 1992, note that the “weak” sample contains strong systems as well). Furthermore, we restrict our analysis to regions of the spectrum which have sufficient signal to noise (s/n) ratio for each sample such that we should be able to detect a 0.3 (0.6) Å rest equivalent width Mg II $\lambda 2796$ line at 3σ significance, which requires $s/n \gtrsim 18(9)$ per 2 Å pixel at 5600 Å. We also exclude the one absorber which lies at a velocity separation $\Delta v < 5000 \text{ km s}^{-1}$ from its background quasar, as it may be an associated Mg II system, rather than intervening. It was also ensured that any pairs of Mg II absorbers along the same line of sight with velocity separation $\Delta v \leq 5000 \text{ km s}^{-1}$ would only be counted as one system, since there is evidence for clustering on that scale (Steidel & Sargent).

3.2. Selection of quasar comparison sample

For comparison with the distribution of Mg II absorbers, we constructed a sample of quasars from Veron-Cetty & Veron (2001) and Keable (1987), Clowes & Campusano (1994) and Clowes, Campusano, & Graham (1999), within a 2.5° radius of RA=10:45:00.0, dec=+05:35:00 (J2000). There are 107 quasars at $0.6 < z < 2.2$, with another 23 at $2.2 < z < 3.3$. They were found via a variety of selection methods, so we use them as fixed reference locations for known mass concentrations in the region. A map of the quasars in the large quasar group and Mg II absorbers in the redshift range $1.20 < z < 1.39$ is in Fig. 3.

3.3. Other metals and candidate damped systems

We searched for other metal absorption lines by cross-correlating a list of metal transition wavelengths with the redshifts of identified Mg II systems, and found a number of Fe II lines, as well as Mg I, Al II, Al III and Mn II. Rao & Turnshek (2000) found that approximately 50% of the absorption systems with $W_0(\text{MgII } \lambda 2796) \geq 0.5 \text{ \AA}$ and $W_0(\text{FeII } \lambda 2600) \geq 0.5 \text{ \AA}$

have damped absorption lines meet the classical definition used in high-redshift surveys, with H I column densities of $N_{HI} > 2 \times 10^{20} \text{ cm}^{-2}$. We have 11 absorption systems with $W_0(\text{MgII } \lambda 2796) \geq 0.5 \text{ \AA}$ and $W_0(\text{FeII } \lambda 2600) \geq 0.5 \text{ \AA}$ in our sample (Table 3), three of which are within the large quasar group. We note that damped Ly α systems themselves often appear to indicate low mass systems (e.g. Fynbo, Møller, & Warren 1999; Warren et al. 2001, and references therein), and thus as a class may trace more typical objects in the universe than brighter, more massive ones as quasars and Lyman break galaxies (e.g. Pettini et al. 2001), though at $z > 2$ the difference may be less clear (Møller et al. 2002). Nevertheless, damped Ly α systems with separations of a few Mpc may trace of large mass concentrations at $z = 2.4$ (Francis et al. 2000) and could prove to be similarly useful at $z \sim 1.2$.

3.4. The peculiar quasar J104642+0531

Among the objects in our sample of quasar spectra, J104642+0531 ($z = 2.681$) is quite puzzling. It is a peculiar background object found serendipitously during a survey in the large quasar group field (Clowes, Campusano, & Graham 1999). There appears to be no C IV emission, but there is extremely broad Ly α emission ($\sim 10^4 \text{ km s}^{-1}$). Clowes et al. found evidence for an associated absorption system at $z = 2.654$, but no O VI or other emission blueward of Ly α . The unusual emission structure merits further study.

4. Tests for large scale structure

We use three methods to test for the presence of a non-random distribution of Mg II systems. First, we calculate the redshift distribution dN/dz , which will reveal whether there are any redshift intervals with anomalously high or low counts of absorbers. Second, we cross-correlate the quasars and Mg II systems in the field. Third, we use the minimal spanning tree test to determine whether Mg II systems form any connected structures.

4.1. Redshift distribution

To calculate the significance of any deviations of the observed Mg II absorber redshift distribution, we created control data samples which, except for clustering, accurately reflect the statistical characteristics of our data. The specific, irregular arrangement of detection windows in redshift space and lines of sight could create a subtle pattern of aliasing to appear

like correlations on certain scales, comparable to the separation between lines of sight and the extent that each spectrum probes along the line of sight. To overcome these difficulties, we produced control samples free of correlations between absorbers. The technique is analogous to one used in a similar study of C IV absorbers at $z \sim 2.4$ (Williger et al. 1996), where a complete description can be found.

We used results from Steidel & Sargent (1992), who performed a Mg II survey toward 103 quasars scattered throughout the sky to parametrize the redshift distribution $dN/dz = N_0(1+z)^\gamma$ where $\gamma = 1.12, 1.17$ for weak, strong systems, $W_0(\lambda 2796) \geq 0.3, 0.6 \text{ \AA}$, and the normalization is $\langle dN/dz \rangle = 0.97, 0.52$ at $\langle z_{abs} \rangle = 1.12, 1.17$ respectively. If we integrate over the redshift range of each of our lines of sight to which we are sensitive to $W_0(\lambda 2796) = 0.3, 0.6 \text{ \AA}$,

$$N = \sum_{i=1}^{n_{quasars}} \int_{z_{low}}^{z_{high}} N_0(1+z)^\gamma dz \quad (1)$$

where the integral runs through each of the lines of sight i from z_{low} to z_{high} , we find a total observed number of absorbers over $0.7 < z < 2.0$ which is overdense at the $\sim 2.3 - 2.4\sigma$ level compared to the Steidel & Sargent statistics for both the weak and strong samples (Table 4).

We used the same parametrization to create 10000 randomized data samples, by associating a particular sightline and redshift with a point in the normalized cumulative redshift density function based on the actual lines of sight and redshift limits. The expected number of Mg II systems is based on a Steidel & Sargent’s sample of 111 weak systems ($\Delta z = 114.2$) and 67 strong ones ($\Delta z = 129.0$). In comparison, our surveys represent roughly one third of the absorbers in about one fifth of the redshift space. The overdensity in absorber number for our sample could be due entirely either to (a) an overdensity at all redshifts (cosmic variance) or (b) the presence of one or more localized significant overdensities. We consider each case.

To account for cosmic variance, the number of Mg II absorbers in each random sample was drawn from a Poissonian distribution with a mean *equal to the number of absorbers actually observed*. For the strong survey, we find no significant deviation from a random distribution (perhaps due to the small sample size). However, for the weak survey, we find an overabundance of Mg II systems at $1.2 < z < 1.4$, which is coincident with the Clowes & Campusano large quasar group: we find 11 absorbers, and expect 5.5 ± 2.2 . The Mg II redshift distribution, our selection function and (for reference) the quasar redshift distribution are shown in Fig. 4a. If we assume a Gaussian distribution for the simulated number of absorbers at $1.2 < z < 1.4$, this would be a significance of 2.5σ . If we measure the probability directly from the number of simulations, 1.78% of any of the 90000 total redshift bins (9 bins \times 10000 simulations) produced an overdensity at the 2.5σ level; 2.05%

had 11 or more absorbers in the $1.2 < z < 1.4$ bin. The large quasar group occupies the same redshift interval, which implies that the Mg II and quasar overdensities are related; in fact, despite the various selection methods used for the quasars, the ratio between quasars and Mg II absorbers remains constant (within Poissonian errors of 1.1σ) over $0.8 < z < 2.0$.

If there is an anomalous concentration of absorbers at a particular redshift, which could be the case if Mg II systems are associated with the large quasar group, then the expected number of Mg II systems in the same redshift range as the large quasar group would be overestimated by the above procedure, and the significance thus underestimated. If we draw 10000 random samples from a Poissonian number distribution with a mean of 24 (which is the expected number from the weak sample given our redshift coverage and the Steidel & Sargent redshift number density), then we would expect 3.4 ± 1.8 Mg II absorbers at $1.2 < z < 1.4$, resulting in a 4.3σ overdensity in that redshift bin (Fig. 4b). Only 0.02% of the simulations produced 11 absorbers in that bin, and 0.01% produced more; only 0.06% of *any* of the 90000 bins in any simulation had a significance of 4.3σ or higher.

A conservative estimate for the significance of the overdensity at $1.2 < z < 1.4$ is therefore 2.5σ , though it could be as high as 4.3σ depending on how we normalize our control sample.

4.2. Quasar-Mg II correlations

To test for quasar-Mg II correlations in three dimensions, we calculated the three dimensional two point correlation function between the 107 quasars at $0.6 < z < 2.2$ in our sample and all of the Mg II absorbers over all redshifts in our survey. We used 10000 control samples with randomized Mg II absorber redshifts similar to those described in the previous section. We found no significant signal for either the strong or weak survey at any scale.

We then tested for correlations in the plane of the sky. Although no such three dimensional large scale correlation has been noted in the literature, there is a precedent for an association between quasars and C IV absorbers at a *projected* distance of ~ 10 Mpc (Møller 1995; private communication). We cross-correlated the same quasars with the strong and weak Mg II samples, but only along *different* lines of sight (which avoids effects from associated absorption) for a series of projected separations on the sky covering $5 - 50h^{-1}$ Mpc in the local frame. Again, we used 10000 control samples with randomized Mg II redshifts, drawing a number from a Poisson distribution with a mean equal to the number of observed absorbers, to determine the mean and standard deviation expected in each bin. As the number of quasar-Mg II pairs varied for each simulated data set, we normalized the total number

of pairs for each simulation to that actually observed. There is no significant signal for the strong sample, but for the weak sample we find a signal which peaks at $9h^{-1}$ proper (rest frame) Mpc projected separation (35 arcmin at $z = 1.2$) at the 3.5σ significance level (8 pairs observed, 2.4 ± 1.6 expected). The overdensity occurs at a velocity difference $\Delta v = -4500$ to -3000 km s^{-1} . The negative sign indicates that a quasar is at a lower redshift than its paired Mg II absorber (Fig. 5; Table 5). We expect the peak to be at $\Delta v \sim 0$ if the quasar redshifts are accurate, and if quasars and Mg II systems trace mass in a similar way. Only 0.23% of the simulations produced as many as 8 pairs in the $\Delta v = -4500$ to -3000 km s^{-1} velocity bin, with 0.26% of *any* bins among all of the Monte Carlo simulations producing an equal or greater overdensity of $\geq 3.5\sigma$. There is no significant preference for strong or weak systems to be associated with the correlation. Most of the signal (i.e. 5 of 8 pairs) comes from quasars and Mg II absorbers in the large quasar group. Possible physical explanations for the overdensity will be discussed in §5.

It is possible, but unlikely, that the quasar-Mg II absorber pair velocity difference is produced by a systematic quasar offset between quasar rest frame UV and optical lines. Our quasar redshifts were taken either from the Veron-Cetty & Veron (2001) catalogue, measured from our own $\sim 10 \text{ \AA}$ confirmation spectra (Clowes & Campusano 1994; Clowes, Campusano, & Graham 1999) or, in the case of 22 of the quasars (all except J104545+0523), from the data presented here. There is no systematic offset between the our two sets of measurements, independent of whether Mg II, C IV, Si IV or C III] emission lines were used. Five of the eight quasar-Mg II pairs at $-4500 < \Delta v < -3000 \text{ km s}^{-1}$ have quasar redshifts determined from Mg II emission lines. The other three are from higher ionization C IV or C III] emission lines. McIntosh et al. (1999) and Scott et al. (2000, and references therein) find that quasar Mg II emission provides redshifts within $\sim 400 \text{ km s}^{-1}$ of [O III] 5007 (the systemic redshift fiducial), with a correlation between velocity differences and quasar luminosity. However, the observed peak in the distribution of quasar-Mg II absorber pairs is at $\Delta v \sim 10$ times larger than would be expected from an offset between Mg II (rest frame UV) and the fiducial [O III] 5007 (rest frame optical) emission. IR spectroscopy of the quasars which produce the quasar-Mg II pair overdensity can confirm or rule out this rather unlikely explanation.

The luminosities of the quasars involved in the correlation are not unusual. The 8 quasars in the overdensity of pairs with $\Delta v = -4500$ to -3000 km s^{-1} have mean absolute magnitude $\langle M_{abs} \rangle = -25.8 \pm 1.0$, calculated with code kindly provided by M. Veron-Cetty for the purposes of using a uniform definition of M_{abs} . Our sample of quasars at $0.6 < z < 2.2$ has $\langle M_{abs} \rangle = -25.7 \pm 1.0$, whereas 16892 quasars in the Veron-Cetty & Veron catalogue at the same z range have $\langle M_{abs} \rangle = -25.4 \pm 2.4$. Our quasar sample is not significantly more luminous than a very large but admittedly inhomogeneous sample, so it is doubtful that a luminosity effect contributes to part of the systematic velocity difference we observe between

the quasars and Mg II absorbers. Indeed, the correlation may simply be a fluke due to small number statistics, and should be confirmed with a larger data sample.

4.3. Minimal spanning tree

The minimal spanning tree (MST) is a heuristic algorithm which can delineate and characterize structure within a data set. We have applied the technique of Graham, Clowes, & Campusano (1995) to search for clusters of Mg II absorbers in both the strong and weak samples. An identified cluster is assigned a statistical significance by determining how frequently structures of equivalent multiplicity¹ and with a more clustered morphology occur in 10000 simulations of the data. A simulated absorber position is assigned the right ascension and declination of a randomly selected real absorber to maintain any selection effects in the plane of the sky. Its redshift is determined according to one of three prescriptions: (1) drawn from the observed redshift distribution binned in bins of width $\Delta z = 0.2, 0.4$; (2) drawn from the Steidel & Sargent (1992) redshift distribution; and (3) as (2) but with the total number count normalized to the observed number count. For (1), the bins were selected either to match the large quasar group width or to double it, to smooth out Poisson fluctuations on scales of half a bin width or smaller. For (2) and (3), cosmic variance is also taken into account as previously described. No significant structures are found in the strong survey, but a cluster of 10 absorbers is found in the weak survey at redshift $z \sim 1.3$. The significance level for the $z \sim 1.3$ structure from prescription (1) is $P = 0.005$ (0.002) for $\Delta z = 0.2$ (0.4); for prescriptions (2) and (3), $P = 0.04, 0.01$ respectively.

Foreground structure at $z \approx 0.8$. At lower redshift, the MST test shows a group of 7 absorbers at $0.77 < z < 0.89$ with probability to reject that the decision to reject the null hypothesis (that the absorbers are intrinsically unclustered) is wrong of $P \approx 0.005 - 0.02$. The exact value of P depends on which of the three prescriptions in the preceding paragraph was used to create the control samples. P is largely independent of the choice of redshift bin width for the controls ($\Delta z = 0.1, 0.2, 0.4$). It appears that at least one of the absorbers is very close (within 1 arcmin) to a galaxy cluster at $z \approx 0.8$ (Haines 2001). There is also a structure of 14 quasars at $z \approx 0.8$, which is consistent with a random distribution with probability $P_{config} = 0.066$ for the observed multiplicity, as determined from a MST analysis of the Chile-UK Quasar Survey (CUQS, Newman 1999). The probability is again independent of control redshift bin widths. The number of quasars from our sample (Newman 1999) is

¹Multiplicity is a term used in spatial pattern statistics to denote the number of objects making up a cluster.

lower at $z < 1$, with the probability of any structure arising at $z < 1$ of $P_{z < 1} = 0.14 - 0.19$. Thus, the probability of seeing the observed structure at $z \approx 0.8$ is $P_{config}P_{z < 1} \sim 0.01$. The coincidence of the Mg II absorber group, the quasar group and its size, and the proximity of a cluster of red galaxies support the notion of a foreground structure.

5. Discussion

The coincidence of the MgII absorber candidate overabundance with the large quasar group implies that the large quasar group is accompanied by a corresponding increase in galaxy density, possibly similar to those found associated with multiple C IV systems at $z \sim 2$ by Aragón-Salamanca et al. (1994). The MST result provides an independent test which supports the existence of a structure of Mg II absorbers within the large quasar group. The quasar-Mg II correlation may reflect a characteristic size of filaments.

5.1. Mg II absorber overdensity

It may be that Mg II absorbers within the large quasar group could be associated with nearby enhanced ionizing sources such as undetected quasars or AGN. In that case, the halos of the galaxies responsible for the Mg II absorption could possess smaller detectable gas cross sections than in the field, the “galaxy proximity effect” (Pascarelle et al. 2001), which would cause us to underestimate the significance of the Mg II absorber (galaxy) number density in the region. Any mass estimates for the region would also have to take into account that numerical simulations and semi-analytic models show that galaxies should be more highly biased tracers of the mass at higher redshift. If so, then the overdensity of matter in galaxies which produce the Mg II absorption could be closer to the overdensity of matter in super large scale structure of 5 – 10 above the mean predicted by Doroshkevich et al. (1999). Estimates of the matter associated with Mg II absorber overdensities could be redshift-dependent: in CDM models, as the amplitude of galaxy clustering remains roughly fixed, the dark matter structure grows with time. Large quasar groups and the galaxies they contain could provide the means to test for such a trend: direct imaging of the Mg II absorbers in the large quasar group should reveal whether there is a tendency for them to occur in areas of higher than average galaxy density, and velocity dispersions of any associated galaxy clusters/groups should constrain the amount of matter in the vicinity. High resolution imaging of Mg II absorbers in the large quasar group could also reveal whether quasars behind the large quasar group are being lensed by galaxies within the large quasar group, which would make it more likely to observe bright background quasars in the region and find foreground Mg II.

Though rare, large structures at $z \sim 1$ have clearly been noted in simulations. Evrard et al. (2001, Hubble volume simulations) find a large cluster at $z = 1.04$ in a Λ CDM model which has a mass twice that of Coma, a line-of-sight velocity dispersion of $\Delta v = 1900$ km s $^{-1}$ and an equivalent X-ray temperature of 17 keV. It is larger than any known cluster. Although unusual, it might be representative of parts of super large scale structure at $z \sim 1$. X-ray observations of our large quasar group field, for example around the merging galaxy clusters imaged in the optical and near IR by Haines et al. (2001), would provide the most direct confirmation for such large density perturbations. If baryonic gas evolution can be linked to the dark matter halos in simulations such as that of the Virgo Consortium (which is admittedly difficult, as Mg II arises in galaxies), it could be possible to make mock pencil-beam surveys through the simulated data, and thus make a direct comparison between the observed and predicted size and frequency of large quasar groups and the distribution of galaxies/Mg II absorbers within them. However, it would be more feasible to study Hubble volume simulations of Ly α absorbers (which do not necessarily arise in galaxies), and to compare their distribution to the presence of very large structures. In that case, a comparison with observations would require HST spectroscopy for our target field.

A possible non-gravitational origin of such large structures as large quasar groups could be the destruction of H $_2$ or the ionization of He, both of which can be affected over one to several tens Mpc by luminous quasars or other effects of “cooperative galaxy formation” (Miralda-Escudé et al. 2000; Ferrara 1998; Bower et al. 1993; Kang & Shapiro 1992; Babul & White 1992). However, enhanced photoionization has been proposed to *impede* galaxy formation, at least for low mass halos, by heating the intergalactic medium, inhibiting the collapse of gas into dark halos and reducing the radiative cooling of gas within halos, though galaxies in deep potential wells (brighter than L_*) appear unaffected (Benson et al. 2001). Large scale perturbations approaching large quasar group size can produce bias on similar size scales, effectively reducing the galaxy formation efficiency in surrounding lower density regions, and thus enhancing the contrast of very large scale structure (Demianski & Doroshkevich 1999). The effect of inhomogeneous photoionization on structure formation clearly deserves further investigation.

5.2. Quasar–Mg II absorber correlation

The quasar-Mg II absorber correlation may reflect the size of LSS filaments, and is close to the 7 Mpc size of filaments associated with low z Ly α forest clouds from simulations of structure evolution (Petitjean, Mückel, & Kates 1995). The angular scale where the peak number of pairs is observed (corresponding to 35 arcmin at $z \approx 1.2$) is consistent with the

correlations of up to 1° between $-24 < M_B < -19$ AGN and early-type galaxies detected by Brown et al. (2001). We note that five of the eight quasar-Mg II system pairs occur within the large quasar group ($1.24 < z < 1.35$). The five large quasar group quasar-Mg II absorber pairs as an ensemble produce most of the significance in the distribution of pairs as a function of velocity (an overdensity at the $\sim 2\sigma$ level), and form a pair and a triplet of quasars of scale $1\text{-}10h^{-1}$ Mpc, a size on the order of that expected for filamentary structure. The peak at $-4500 < \Delta v < -3000$ km s $^{-1}$ should be confirmed with IR spectroscopy of the quasars in question, to rule out the unlikely possibility that the large velocity difference arises from high *vs.* low ionization line emission regions. Otherwise, the quasars and MgII systems could trace different parts of the same filamentary substructure within the large quasar group. Such a geometry may result as a consequence of the “periphery effect”, in which quasars tend to populate the peripheries of galaxy clusters and metal absorption line groups (Jakobsen & Perryman 1992; Sánchez & González-Serrano 1999; Tanaka et al. 2000; Haines et al. 2001; Söchting, Clowes, & Campusano 2002). In a particularly analogous situation to the large quasar group in this study, Tanaka et al. (2001) detect clustering of faint red galaxies ($I > 21$, $R - I > 1.2$) over a scale extending to $10 h^{-1}$ Mpc around a tight group of five radio-quiet quasars at $z \sim 1.1$, which are embedded in the Crampton, Cowley, & Hartwick (1987, 1989) large quasar group of 23 quasars. Haines et al. (2001) report a similar phenomenon around the $z \approx 1.23$ quasar J104656+0541 within the large quasar group studied here, albeit in a smaller observed field.

If the periphery effect is the cause of our observed quasar-Mg II correlation at non-zero velocity difference, then we should in principle detect a signal at both positive and negative Δv (according to our definition). However, we only see a negative velocity peak, in which the largest fraction of the signal arises from a set of quasars at $z = 1.236, 1.273, 1.316$ separated by $36.9 \times 34.3 \times 52.2$ arcmin and $4900, 5600$ km s $^{-1}$ in front of a trio of Mg II absorbers separated by $5100, 5700$ km s $^{-1}$ toward two sightlines 29.8 arcmin apart. If the correlation is real, in larger data samples we would expect to find cases of quasars both in front of and behind groups of Mg II absorbers. Alternatively, such a quasar-Mg II correlation which arises for projected distances on the sky, but not in three dimensions, could arise as an effect of peculiar velocities along the line of sight, and may be related to the “bull’s-eye effect” (Praton, Melott, & McKee 1997; Melott et al. 1998), in which peculiar velocities in collapsing structures tend to make structures more significant in redshift space than in real space. The number of quasar-Mg II pairs in the large quasar group is not sufficient to produce a significant signal on its own, however, and the correlation should be confirmed with a larger sample.

If the quasar-Mg II projected correlation is found to be real, it could be a useful tool to probe the extent and evolution of the overdensities giving rise to quasars themselves. It is

possible that quasar clustering declines toward low redshift, as quasar activity moves from the most massive galaxies into lower mass systems that are less highly biased. We expect to continue to find more members of the large quasar group toward ESO/SERC field 927, which will provide better statistics with which to study the relationship between various matter overdensities in the form of quasars, Mg II systems and galaxies.

We thank Romeel Davé, Andrei Doroshkevich, Gus Evrard, Dick Hunstead, Palle Møller, Martin Rees, Steve Warren, David Weinberg and Simon White for useful discussions and comments on a draft of this paper, Robert Hill for data reduction software and Alvaro Amigo for assistance with the data reduction. We also thank the anonymous referee for helpful suggestions concerning the clarity of our presentation and results.

REFERENCES

- Aragón-Salamanca, A., Ellis, R. S., Schwartzberg, J.-N., Bergeron, J. A. 1994, *ApJ*, 421, 27
- Babul, A. & White, S. D. M. 1991, *MNRAS*, 253, 31P
- Benson, A. J., Lacey, C. G., Bauth, C. M., Cole, S., & Frenk, C. S. 2001, *MNRAS*, submitted, astro-ph/0108217
- Best, J. S. 2000, *ApJ*, 541, 519
- Bower, R. G., Coles, P., Frenk, C. S., & White, S. D. M. 1993, *ApJ*, 405, 403
- Brown, M. J. I., Boyle, B. J., & Webster, R. L. 2001, *AJ*, 122, 26
- Cen, R. & Simcoe, R. A. 1997, *ApJ*, 483, 8
- Davé, R., Hernquist, L., Katz, N., Weinberg, D. H. 1999, *ApJ*, 511, 521
- Clowes, R. G. 2001, in, “The New Era of Wide Field Astronomy”, Clowes, R. G., Adamson, A., Bromage, G. eds., San Francisco, Astron. Soc. Pacific, ASP Conf Series, Vol. 232.
- Clowes, R. G. & Campusano, L. E. 1991, *MNRAS*, 249, 218
- Clowes, R. G. & Campusano, L. E. 1994, *MNRAS*, 266, 317
- Clowes, R. G., Campusano L. E., & Graham M. J. 1995, in Maddox S. J., Aragón-Salamanca A., eds, The 35th Herstmonceux Conference, Wide Field Spectroscopy and the Distant Universe. World Scientific Publishing, Singapore, p. 400

- Clowes, R. G., Campusano, L. E., & Graham, M. J. 1999, MNRAS, 309, 48
- Crampton D., Cowley A.P., & Hartwick F.D.A. 1987, ApJ, 314, 129
- Crampton D., Cowley A.P., & Hartwick F.D.A. 1989, ApJ, 345, 59
- Demianski, M. & Doroshkevich, A. G. 1999, ApJ, 512, 527
- Demianski, M. & Doroshkevich, A. G. 2000, MNRAS, 318, 665
- Doroshkevich, A. G., Fong, R., McCracken, H. J., Ratcliffe, A., Shanks, T., Turchaninov, V. I. 2000, MNRAS, 315, 767
- Doroshkevich, A. G., Müller, V., Retzlaff, J., Turchaninov, V. L. 1999, MNRAS, 306, 575
- Evrard, A. E. et al. 2001, ApJ, submitted, astro-ph/0110246
- Ferrara, A. 1998, ApJ, 499, L17
- Francis, P. J., Williger, G. M., Collins, N. R. et al. 2001, ApJ, 554, 1001
- Fynbo, J. U., Møller, P., & Warren, S. J. 1999, MNRAS, 305, 849
- Geller, M. J. et al. 1997, AJ, 114, 2205
- Guillemin, P. & Bergeron, J. 1997, A&A, 328, 499
- Graham, M. J., Clowes R. G., & Campusano L. E. 1995, MNRAS 275, 790
- Haines, C. P. 2001, PhD Thesis, Univ. of Central Lancashire
- Haines, C. P., Clowes, R. G., Campusano, L. E., Adamson, A. J. 2001, MNRAS, 323, 688
- Jakobsen, P. & Perryman, M. 1992, ApJ, 392, 432
- Kang, J. & Shapiro, P. R. 1992, ApJ, 386, 432
- Keable, C. J. 1987, PhD Thesis, Univ. Edinburgh
- Komberg, B. V. & Lukash, V. N. 1994, MNRAS, 269, 277
- Miralda-Escudé, J., Haehnelt, M, & Rees, M. J. 2000, ApJ, 530, 1
- McIntosh, D.H., Rix, H.-W., Rieke, M.J., & Foltz, C.B. 1999, ApJ, 517, L73
- Melott, A. L., Coles, P., Feldman, H. A. & Wilhite, B. 1998, ApJ, 496, L85

- Miralda-Escudé, J., Haehnelt, M., & Rees, M. J. 2000, *ApJ*, 530, 1
- Møller, P. 1995, in “Galaxies in the Young Universe”, eds. Hippelein, H., Meisenheimer, K., Röser, H.-J., Springer-Verlag, Heidelberg, Lecture Notes in Physics, V. 463, p. 106
- Møller, P., Warren, S. J., Fall, S. M., Fynbo, J. U., Jakobsen, P. 2002, *ApJ*, in press, astro-ph/0203361
- Newman, P. R. 1999, PhD thesis, Univ. of Central Lancashire
- Newman, P. R., Clowes, R. G., Campusano, L. E., Graham, M. J. 1998, 14th IAP Astrophys Coll, Éditions Frontières, p. 408
- Pascarella, S. M., Lanzetta, K. M., Chen, H.-W., Webb, J. K. 2001, *ApJ*, 560, 101
- Petitjean, P., Mückel, J.P., & Kates, R.E. 1995, *A&A*, 295, L9
- Pettini, M. et al. 2001, *ApJ*, 554, 981
- Praton, E. A., Melott, A. L., & McKee, M. Q. 1997, *ApJ*, 479, 15
- Quashnock, J. M., vanden Berk, D. E., & York, D. G. 1996, *ApJ*, 472, L69
- Quashnock, J. M. & Stein, M. L. 1999, *ApJ*, 515, 506
- Rao, S. M., & Turnshek, D. A. 2000, *ApJS*, 130, 1
- Sánchez, S. & González-Serrano, J. 1999, *A&A*, 352, 383
- Scott, J., Bechtold, J., Dobrzycki, A., Kulkarni, V. P. 2000, *ApJS*, 130, 67
- Silk, J. & Weinberg, D. 1991, *Nature*, 350, 272
- Söchtig, I. K., Clowes, R. G., & Campusano, L. E., 2002, *MNRAS*, 331, 569
- Steidel, C.C. & Sargent, W.L.W. 1992, *ApJS*, 80, 1
- Steidel, C. C., Dickinson, M., Meyer, D. M., Adelberger, K. L., Sembach, K. R. 1997, *ApJ*, 480, 568
- Tanaka, I., Yamada, T., Aragón-Salamanca, A., Kodama, T., Miyaji, T., Ohta, K., Arimoto, N. 2000, *ApJ*, 528, 123
- Tanaka, I., Yamada, T., Turner, E. L., & Suto, Y. 2001, *ApJ*, 547, 521
- Véron-Cetty, M.-P., & Veron, P. 2001, *A&A*, 374, 92

Warren, S. J., Møller, P., Fall, S. M., & Jakobsen, P. 2001, MNRAS, 326, 759

Webster, A. 1982, MNRAS, 199, 683

Williger, G. M., Hazard, C., Baldwin, J.A. & McMahon, R.G., 1996, ApJ Supp, 104, 145

Fig.1: (a-f) Spectra in the quasar sample. The 1σ error is shown by the solid line close to the bottom of each plot. The dashed and dotted lines show the wavelengths used for the strong and weak Mg II surveys, respectively. Regions deemed affected by telluric absorption are shaded. Absorption lines are indicated by ticks above the spectrum at $\geq 5\sigma$ (solid) and $2.5 < \sigma < 5$ (dashed) significance; in the telluric bands, only identified extragalactic features are ticked. However, all absorption features are listed in Table 2.

Fig. 1.—

Fig.2: (a-d) Plots of the Mg II doublets in velocity space. Normalized fluxes are shown. The λ 2803 component is shown offset by -0.2 in flux for clarity. The 1σ error array is indicated by the dot-dashed line. The background quasar is listed to the bottom left of each plot, the Mg II absorption redshift is at the bottom center, and four letters indicating the strength of the line (s=strong, w=weak, v=very weak), whether the absorber is in the strong and weak surveys (y/n) and the reality of the system (r=real, c=candidate, d=doubtful), as listed in Table 3. Only “real” systems which are in the strong or weak surveys are used in the analysis for this work.

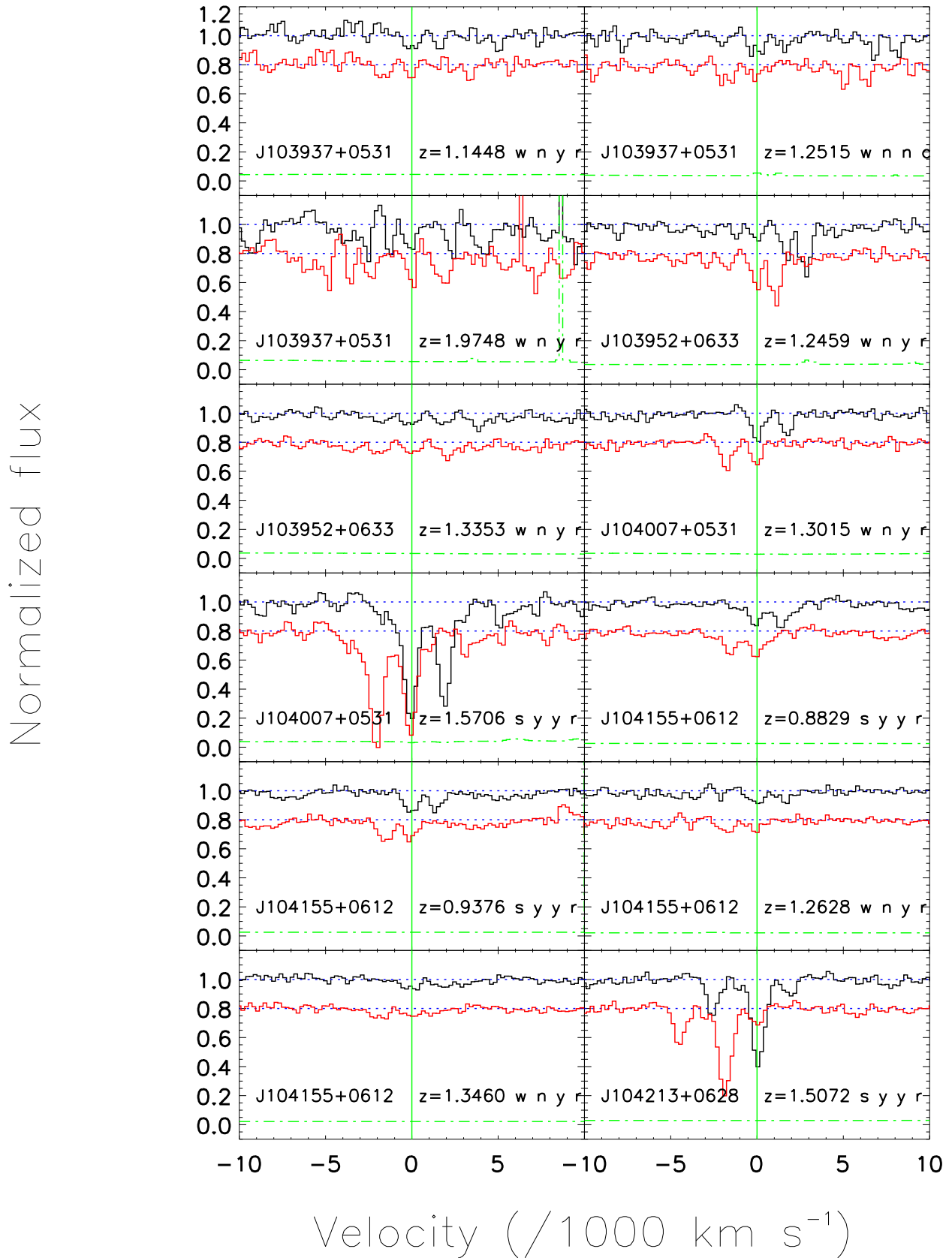


Fig. 2.— (a)

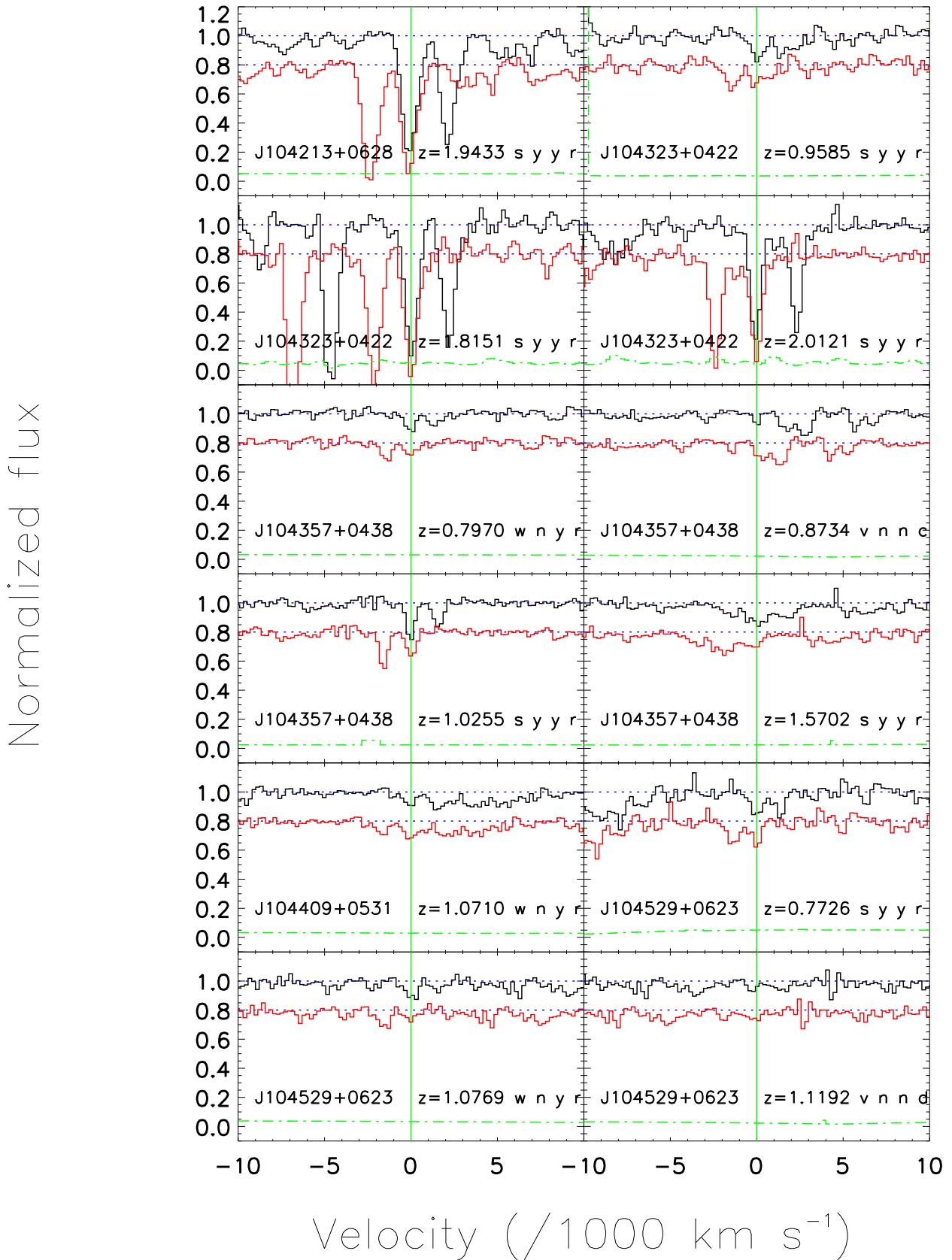


Fig. 2.— (b)

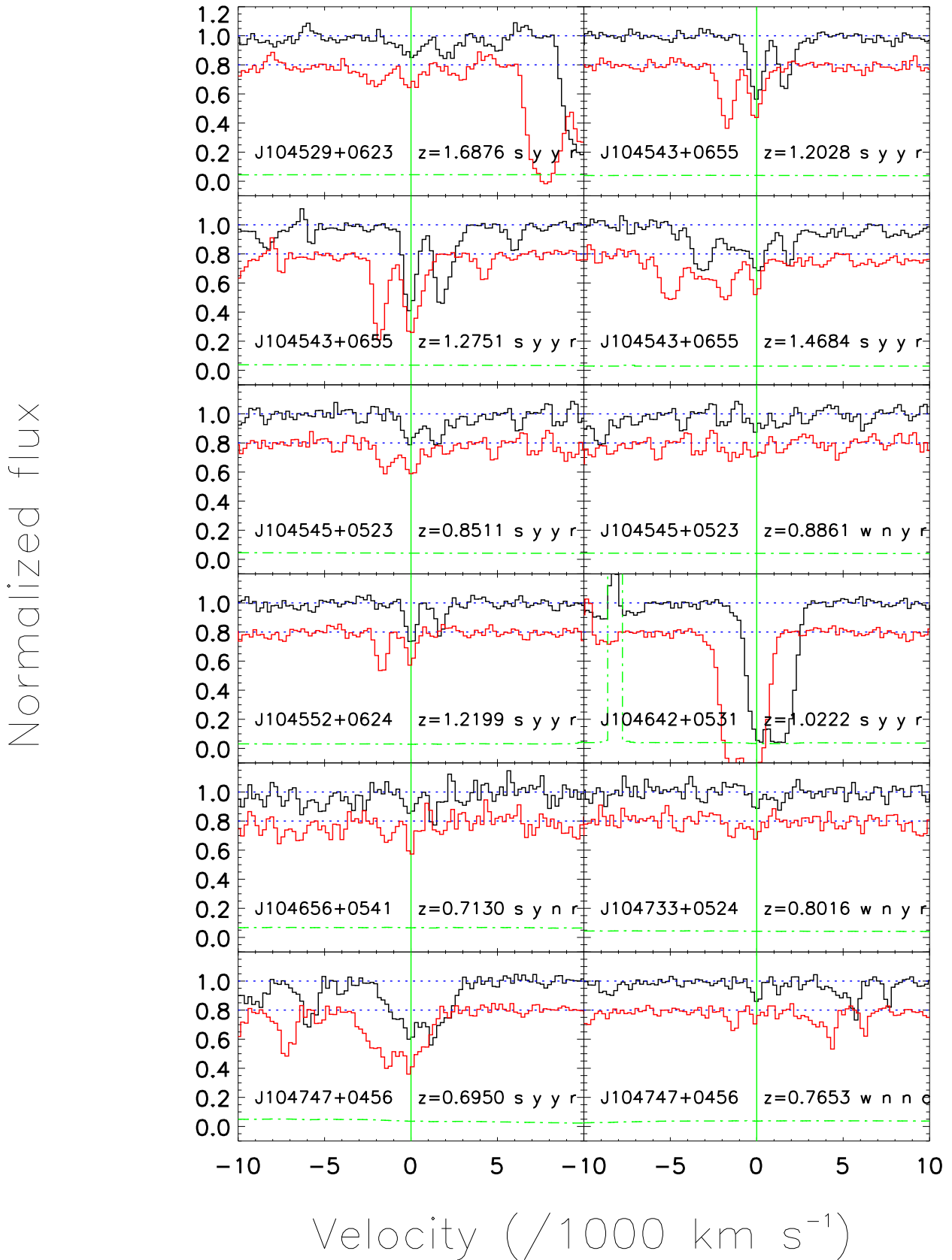


Fig. 2.— (c)

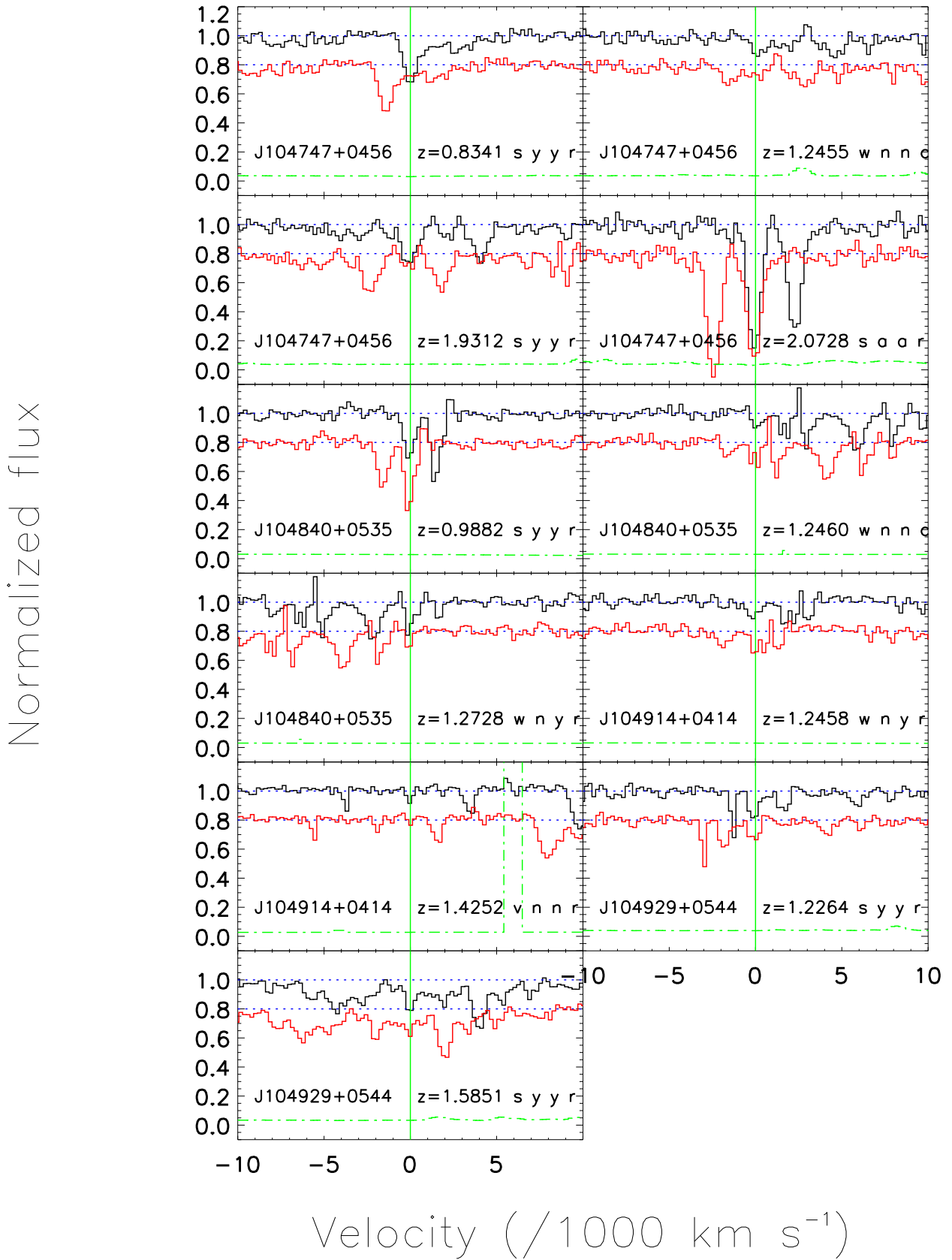


Fig. 2.— (d)

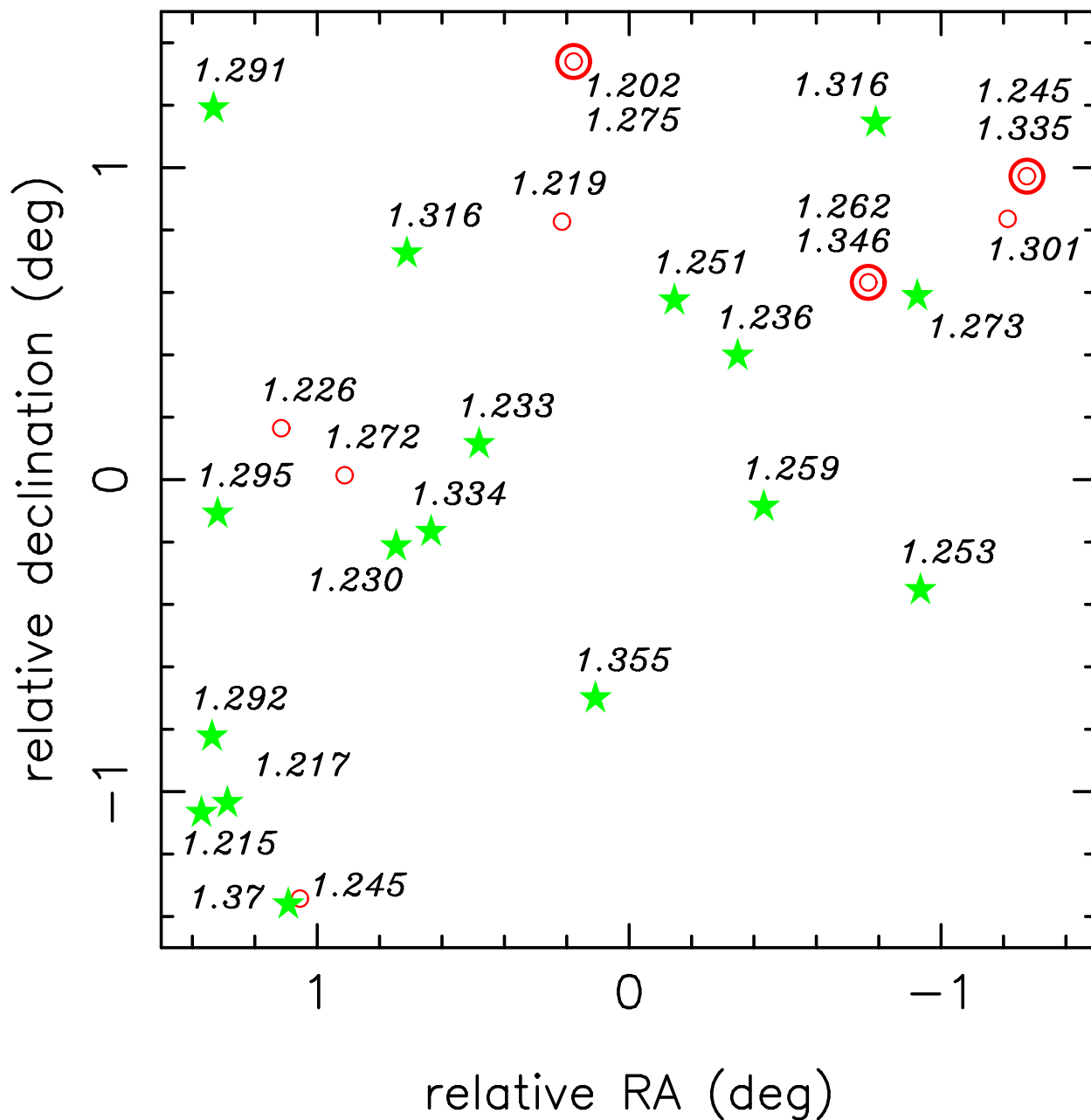


Fig. 3.— Map of the quasars (stars) and Mg II absorbers (circles), at $1.20 < z < 1.39$ toward the Clowes & Campusano large quasar group. *Stars* indicate positions of QSOs in the redshift range $1.20 < z < 1.39$. *Circles* indicate the positions of quasars with $z > 1.39$ with Mg II absorption at $1.20 < z < 1.39$. Double circles indicate two Mg II systems toward a line of sight. Redshifts for the quasars (stars) and Mg II absorbers (circles) are listed adjacent to each symbol. The field center is at RA=10:45:00.0, dec=+05:35:00 (J2000). About half of the structure is shown.

Fig.4: (a) Redshift distribution of the weak Mg II absorber sample, compared to simulations of the number observed. *Filled circles*: observed, with errors assuming a Poissonian distribution. *Dashed line*: mean expected number per bin from 10000 Monte Carlo simulations, drawn from samples with mean totals equal to the number observed (38). *Shaded regions*: 68, 95, 99% scatter about the expected mean. The overdensity at $1.2 < z < 1.4$, which coincides with the large quasar group, was matched or exceeded in 2.05% of the simulations. *Open boxes (slightly offset in z for clarity)*: known quasars in the field, with errors assuming a Poissonian distribution.

(b) Redshift distribution of the weak Mg II absorber sample, compared to simulations of the number expected. *Filled circles*: observed, with errors assuming a Poissonian distribution. *Dashed line*: mean expected number per bin from 10000 Monte Carlo simulations, drawn from samples with mean totals equal to the number expected (24). *Shaded regions*: 68, 95, 99% scatter about the expected mean. The overdensity at $1.2 < z < 1.4$ was matched or exceeded in 0.02% of the simulations. *Open boxes (slightly offset in z for clarity)*: known quasars in the field, with errors assuming a Poissonian distribution.

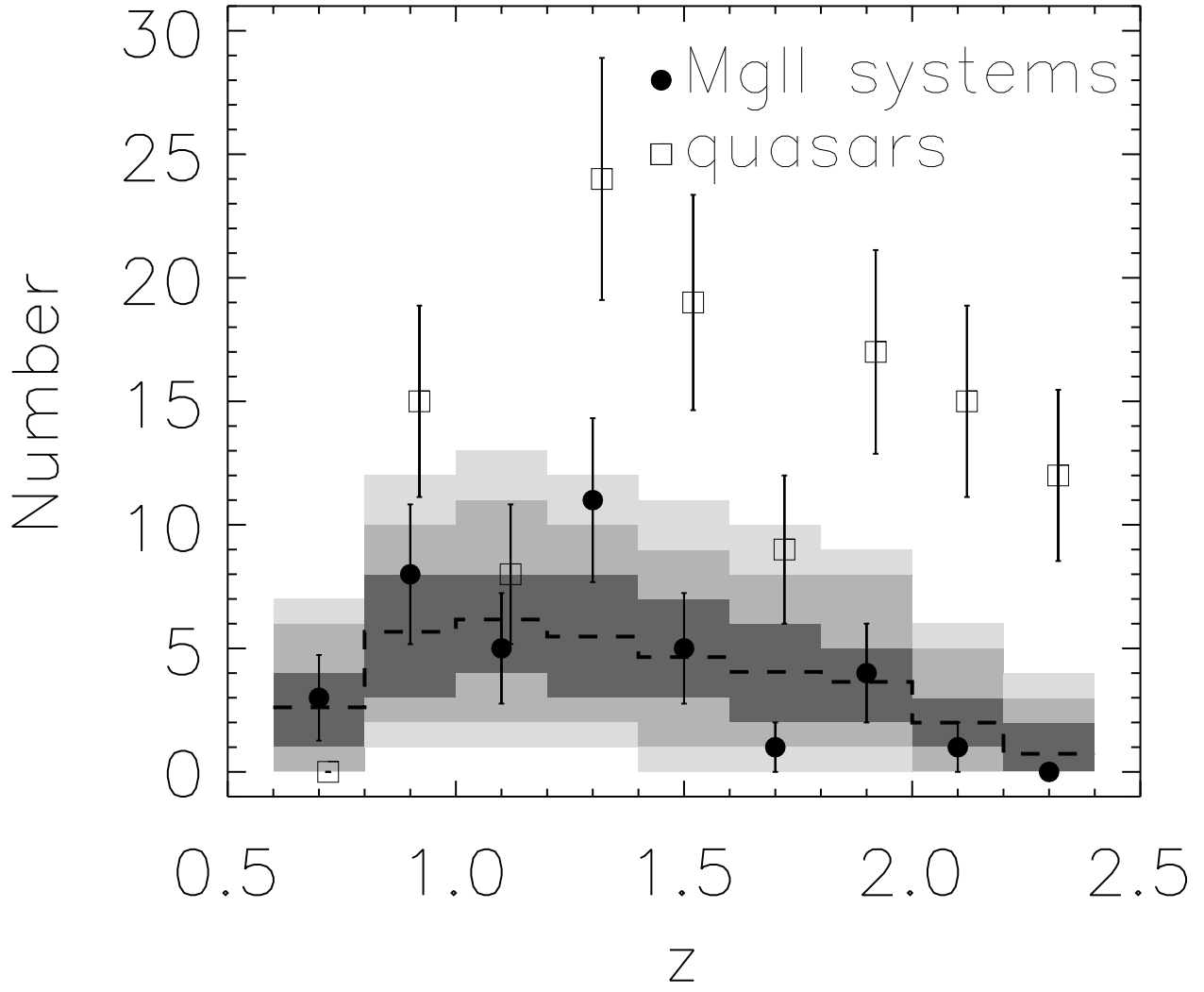


Fig. 4.— (a)

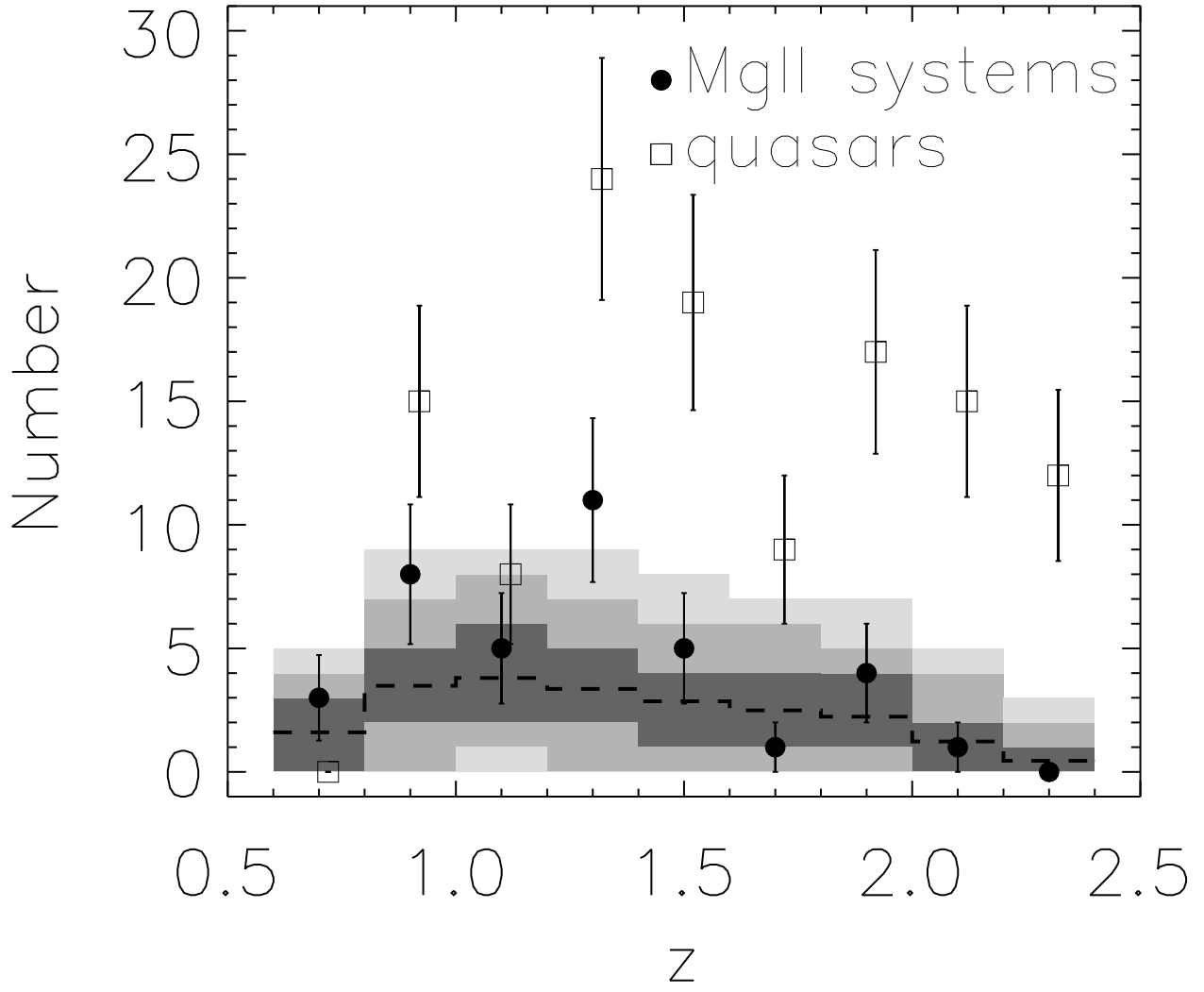


Fig. 4.— (b)

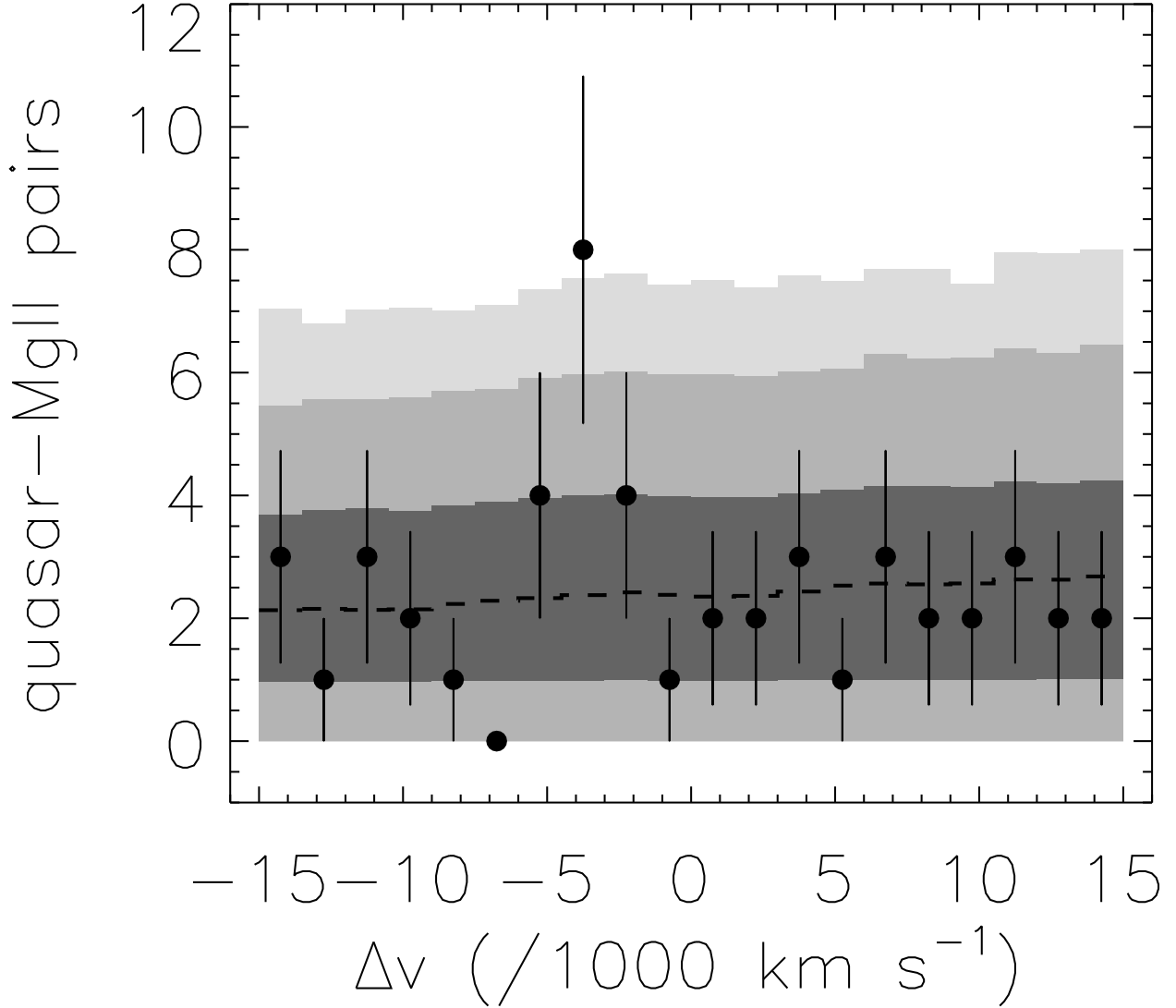


Fig. 5.— Velocity distribution of quasar-Mg II pairs at $9h^{-1}$ Mpc projected separation. Only pairs along *different* lines of sight are counted. Negative velocity differences correspond to the quasar being at lower redshift than the Mg II absorber. *Dashed line*: mean expected number from 10000 Monte Carlo simulations; *Shaded regions, darkest to lightest*: 68%, 95%, 99% limits for the scatter about the expected mean; *Filled circles*: observed data, with error bars drawn assuming a Poissonian distribution as an illustration. The errors are not exactly Poissonian, as any individual quasar or Mg II system could contribute to more than one pair. However, as $9h^{-1}$ Mpc corresponds to 35 arcmin at $z = 1.2$, there are relatively few pairs sharing quasars or Mg II absorbers, so the Poissonian approximation should give a reasonable error estimate. Note the overdensity at $-4500 < \Delta v < -3000$ km s $^{-1}$, which has a random probability of occurrence of $P = 0.002$.

Table 1. Target list / Observing log

quasar	RA J2000	dec J2000	z_Q	U	B	V	R	I	N^a	exp ^b (s)
J103937+0531	10:39:37.2	05:31:46	2.035	18.20	19.13	19.17	18.88	18.11	5 ^d	9899
J103952+0633	10:39:52.2	06:33:22	1.395	18.14	18.90	18.73	18.19	18.13	4 ^d	5790
J104007+0531	10:40:07.5	06:25:09	2.383	18.05	18.54	1 ^c	2400
J104117+0610	10:41:17.1	06:10:17	1.273	15.42	17.03	1 ^c	900
J104155+0612	10:41:55.7	06:12:57	1.480	18.21	19.28	3 ^d	5800
J104213+0628	10:42:13.5	06:28:53	2.031	18.50	19.27	19.21	19.22	18.22	3 ^d	6600
J104213+0619	10:42:13.6	06:19:42	1.560	18.73	19.24	19.09	18.60	17.87	2 ^d	5700
J104323+0422	10:43:23.6	04:22:17	2.338	19.08	18.92	18.89	18.66	17.89	1 ^c	3000
J104357+0438	10:43:57.8	04:38:23	2.409	18.33	18.60	18.63	18.38	17.98	3 ^d	6000
J104409+0531	10:44:09.5	05:31:34	2.110	...	17.95	1 ^c	1500
J104529+0623	10:45:29.8	06:23:39	2.127	18.37	19.16	19.22	18.88	18.17	3 ^d	9600
J104543+0655	10:45:43.6	06:55:24	2.121	18.91	19.29	19.08	18.46	17.58	7 ^d	10696
J104545+0523	10:45:45.8	05:23:55	1.751	19.11	...	18.37	18.08	17.96	2 ^d	2500
J104552+0624	10:45:52.7	06:24:36	1.508	17.27	17.88	18.00	17.60	17.26	1 ^c	1500
J104642+0531	10:46:42.9	05:31:06	2.681	19.58	19.18	18.85	18.23	17.52	1 ^c	3600
J104656+0541	10:46:56.7	05:41:49	1.233	17.56	18.28	18.14	17.88	17.39	1 ^c	1500
J104733+0524	10:47:33.2	05:24:55	1.334	16.84	17.87	1 ^c	1500
J104747+0456	10:47:47.1	04:56:37	2.121	18.54	19.21	19.24	18.98	18.08	1 ^c	3600
J104752+0618	10:47:52.7	06:18:28	1.316	18.28	19.12	19.16	18.56	18.18	2 ^d	4800
J104840+0535	10:48:40.1	05:35:50	1.972	17.69	18.66	18.68	18.49	17.89	3 ^d	5100
J104914+0414	10:49:14.3	04:14:27	1.613	18.61	19.07	19.04	18.79	18.25	2 ^d	5500
J104929+0544	10:49:29.1	05:44:53	1.802	18.77	19.07	18.97	18.57	18.02	1 ^c	3000
J105010+0432	10:50:10.1	04:32:48	1.217	17.71	18.42	18.33	18.01	17.66	1 ^c	2400

^anumber of exposures

^btotal exposure time

^cobserved during run 1 (1997 March 30 - April 1)

^dobserved during run 1 and run 2 (1999 March 23-24)

Table 2. Absorption line list for quasars

Central wavelength λ (Å, vacuum)	$\Delta\lambda^a$	Equivalent width W (Å)	ΔW	signif ^b	identification /comments ^{c,d}
J103937+0531					
5569.69	0.87	1.543	0.232	6.651	
5583.63	0.51	2.014	0.221	9.113	
5681.09	1.17	1.709	0.249	6.863	
5997.72	1.03	0.733	0.218	3.362	Mg II 2796 $z = 1.1448$
6012.73	0.87	0.471	0.177	2.661	Mg II 2803 $z = 1.1448$
6295.94	0.71	1.112	0.228	4.877	Mg II 2796 $z = 1.2515?$ (bl)
6314.80	1.27	0.455	0.167	2.725	Mg II 2803 $z = 1.2515?$ (bl)
6358.44	0.51	0.879	0.155	5.671	
6874.77	0.26	4.527	0.189	23.952	λ_{\oplus}
6893.81	0.41	2.074	0.165	12.570	λ_{\oplus}
6907.73	0.42	1.717	0.155	11.077	λ_{\oplus}
6933.59	1.08	1.261	0.197	6.401	
7173.06	0.80	1.520	0.212	7.170	λ_{\oplus}
7187.23	0.44	1.570	0.171	9.181	λ_{\oplus}
7197.53	0.40	1.372	0.158	8.684	λ_{\oplus}
7207.79	0.61	1.148	0.174	6.598	λ_{\oplus}
7234.03	1.03	1.401	0.227	6.172	λ_{\oplus}
7252.61	0.56	2.257	0.219	10.306	λ_{\oplus}
7265.42	0.42	1.350	0.163	8.282	λ_{\oplus}
7281.63	0.48	1.196	0.166	7.205	λ_{\oplus}
7291.23	0.77	1.023	0.196	5.219	λ_{\oplus}
7350.18	0.68	0.963	0.190	5.068	
7607.40	0.22	17.027	0.405	42.042	λ_{\oplus}
7626.89	0.16	5.146	0.233	22.086	λ_{\oplus}
7645.18	0.36	12.443	0.435	28.605	λ_{\oplus}
7923.77	0.60	3.340	0.347	9.625	Mg II 2796 $z = 1.8323?$ (bl; 2803 cpt very weak)
7971.77	0.49	1.906	0.272	7.007	
8000.41	0.57	2.582	0.322	8.019	Mg II 2796 $z = 1.8623?$ (bl; 2803 cpt very weak)
8163.49	1.07	2.886	0.446	6.471	λ_{\oplus}
8232.15	0.80	1.710	0.337	5.074	λ_{\oplus}
8318.53	1.34	1.297	0.335	3.872	Mg II 2796 $z = 1.9748$

Table 2—Continued

Central wavelength λ (Å, vacuum)	$\Delta\lambda^a$	Equivalent width W (Å)	ΔW	signif ^b	identification /comments ^{c,d}
8339.77	0.64	1.114	0.248	4.492	Mg II 2803 $z = 1.9748$
8357.90	0.92	2.007	0.356	5.638	
8407.43	0.65	1.850	0.296	6.250	
8423.14	0.60	1.415	0.247	5.729	
8440.43	0.79	1.878	0.288	6.521	
8471.81	0.74	1.373	0.253	5.427	
8767.05	0.75	3.976	0.516	7.705	
J103952+0633					
5840.62	0.60	0.553	0.143	3.867	Fe II 2600 $z = 1.2459$
5873.53	1.30	1.185	0.223	5.314	
6280.34	0.81	0.739	0.173	4.272	Mg II 2796 $z = 1.2459$
6296.15	0.48	1.522	0.181	8.409	Mg II 2803 $z = 1.2459$ (bl)
6306.73	0.37	2.333	0.252	9.258	
6529.33	1.30	0.792	0.198	4.000	Mg II 2796 $z = 1.3353$
6547.39	0.97	0.726	0.174	4.172	Mg II 2803 $z = 1.3353$
6567.63	1.08	1.209	0.205	5.898	
6873.75	0.45	2.475	0.214	11.565	λ_{\oplus}
7253.49	1.12	1.773	0.288	6.156	λ_{\oplus}
7607.59	0.22	15.994	0.390	41.010	λ_{\oplus}
7631.31	0.21	8.257	0.299	27.615	λ_{\oplus}
7650.74	0.42	8.467	0.389	21.766	λ_{\oplus}
8374.97	0.61	1.626	0.285	5.705	
J104007+0531					
4662.20	0.60	0.975	0.254	3.839	Mg I 2026 $z = 1.3015?$
4672.59	0.65	1.997	0.324	6.164	
4683.31	0.85	1.885	0.348	5.417	
4894.71	0.60	1.912	0.332	5.759	
4910.54	0.36	7.504	0.428	17.533	
4926.65	0.27	6.961	0.366	19.019	
4942.36	0.65	5.242	0.452	11.597	
5005.92	0.85	10.295	0.608	16.933	
5042.72	1.01	2.400	0.383	6.266	

Table 2—Continued

Central wavelength λ (Å, vacuum)	$\Delta\lambda^a$	Equivalent width W (Å)	ΔW	signif ^b	identification /comments ^{c,d}
5076.51	0.51	1.792	0.267	6.712	
5091.45	1.03	4.521	0.447	10.114	
5199.92	0.47	5.376	0.275	19.549	
5985.62	1.64	0.679	0.242	2.806	Fe II 2600 $z = 1.3015?$
6025.13	0.52	2.492	0.249	10.008	Fe II 2344 $z = 1.5706$
6125.02	0.29	3.566	0.227	15.709	Fe II 2383 $z = 1.5706$
6279.74	0.80	1.002	0.199	5.035	
6436.51	0.49	1.302	0.157	8.293	Mg II 2796 $z = 1.3015$
6452.25	0.38	0.980	0.128	7.656	Mg II 2803 $z = 1.3015$
6648.69	0.38	2.137	0.199	10.739	Fe II 2587 $z = 1.5706$
6669.82	0.49	1.992	0.213	9.352	
6683.70	0.34	3.355	0.220	15.250	Fe II 2600 $z = 1.5706$
6874.18	0.34	3.403	0.222	15.329	λ_{\oplus}
6894.76	0.84	2.118	0.258	8.209	λ_{\oplus}
7185.86	0.33	8.898	0.296	30.061	Mg II 2796 $z = 1.5706$ (bl) λ_{\oplus}
7206.79	0.27	7.317	0.260	28.142	Mg II 2803 $z = 1.5706$ λ_{\oplus}
7239.46	1.14	1.541	0.305	5.052	λ_{\oplus}
7607.35	0.16	16.446	0.271	60.686	λ_{\oplus}
7642.49	0.29	18.384	0.358	51.352	λ_{\oplus}
7682.27	0.78	2.952	0.286	10.322	
8231.52	0.71	2.153	0.266	8.094	λ_{\oplus}
8990.29	0.74	2.965	0.381	7.782	λ_{\oplus}
9006.93	0.80	2.159	0.376	5.742	λ_{\oplus}
9086.04	0.89	1.573	0.304	5.174	λ_{\oplus}
9178.15	0.44	1.199	0.232	5.168	λ_{\oplus}
J104117+0610					
4941.03	0.28	0.791	0.126	6.278	
6874.27	0.29	5.115	0.186	27.500	λ_{\oplus}
6892.20	0.26	2.392	0.133	17.985	λ_{\oplus}
6907.82	0.36	2.859	0.162	17.648	λ_{\oplus}
6923.93	0.39	1.062	0.120	8.850	
6934.03	0.43	0.933	0.116	8.043	
6942.85	0.36	0.835	0.105	7.952	
6954.61	0.61	1.515	0.160	9.469	

Table 2—Continued

Central wavelength λ (Å, vacuum)	$\Delta\lambda^a$	Equivalent width W (Å)	ΔW	signif ^b	identification /comments ^{c,d}
6997.40	0.69	1.521	0.165	9.218	
7022.00	0.68	0.936	0.138	6.783	
7174.44	0.54	1.485	0.155	9.581	λ_{\oplus}
7189.29	0.35	1.811	0.138	13.123	λ_{\oplus}
7204.02	0.51	1.834	0.163	11.252	λ_{\oplus}
7237.41	0.67	0.705	0.137	5.146	λ_{\oplus}
7278.62	0.68	1.151	0.169	6.811	λ_{\oplus}
7292.02	0.72	0.820	0.146	5.616	λ_{\oplus}
7308.47	0.83	0.874	0.157	5.567	λ_{\oplus}
7566.52	0.91	0.803	0.159	5.050	
7607.47	0.10	16.496	0.188	87.745	λ_{\oplus}
7640.97	0.22	16.928	0.260	65.108	λ_{\oplus}
7673.15	0.40	1.109	0.129	8.597	λ_{\oplus}
7683.59	0.57	0.810	0.133	6.090	
8152.73	0.88	1.473	0.224	6.576	λ_{\oplus}
8167.96	0.74	1.225	0.196	6.250	λ_{\oplus}
8182.55	0.66	1.162	0.190	6.116	λ_{\oplus}
8233.64	0.43	2.685	0.222	12.095	λ_{\oplus}
8295.65	0.48	1.358	0.226	6.009	λ_{\oplus}
8324.75	1.17	1.392	0.257	5.416	
8992.45	0.37	1.456	0.235	6.196	λ_{\oplus}
9157.19	0.86	2.007	0.333	6.027	λ_{\oplus}
J104155+0612					
4617.26	0.92	0.864	0.196	4.408	Fe II 2383 $z = 0.9376$ (bl)
5262.48	0.69	1.756	0.174	10.092	Mg II 2796 $z = 0.8829$ (bl)
5279.90	0.54	1.946	0.165	11.794	Mg II 2803 $z = 0.8829$
5417.93	0.46	1.384	0.138	10.029	Mg II 2796 $z = 0.9376$
5432.21	0.71	1.222	0.151	8.093	Mg II 2803 $z = 0.9376$
5531.16	0.66	0.804	0.131	6.137	Mg I 2852 $z = 0.9376$ (bl)
5561.91	0.89	0.671	0.130	5.162	
5887.21	0.85	0.958	0.141	6.794	
5906.31	0.69	0.540	0.107	5.047	λ_{\oplus}
6327.06	0.62	0.849	0.115	7.383	Mg II 2796 $z = 1.2628$
6342.97	0.88	0.725	0.123	5.894	Mg II 2803 $z = 1.2628$

Table 2—Continued

Central wavelength λ (Å, vacuum)	$\Delta\lambda^a$	Equivalent width W (Å)	ΔW	signif ^b	identification /comments ^{c,d}
6559.49	0.88	0.742	0.126	5.889	Mg II 2796 $z = 1.3460$
6576.77	0.98	0.559	0.118	4.737	Mg II 2803 $z = 1.3460$
6875.11	0.24	3.649	0.138	26.442	λ_{\oplus}
6896.83	0.98	1.504	0.159	9.459	λ_{\oplus}
7607.47	0.20	15.239	0.292	52.188	λ_{\oplus}
7642.19	0.35	17.754	0.374	47.471	λ_{\oplus}
7800.37	0.76	0.972	0.184	5.283	
8164.86	0.95	1.709	0.257	6.650	λ_{\oplus}
8200.24	1.16	1.478	0.271	5.454	λ_{\oplus}
8230.23	0.63	2.309	0.253	9.126	λ_{\oplus}
8770.24	0.49	1.960	0.279	7.025	
8891.98	1.12	2.581	0.417	6.189	
8991.11	0.72	3.068	0.385	7.969	λ_{\oplus}
9014.77	1.56	2.473	0.477	5.184	λ_{\oplus}
J104213+0628					
4636.78	0.35	3.847	0.259	14.853	
4648.04	0.45	3.781	0.245	15.433	
4669.49	0.74	0.833	0.153	5.444	
4729.72	0.86	2.936	0.292	10.055	Fe II 1608 $z = 1.9433$ (bl)
4917.36	0.52	2.589	0.232	11.159	Al II 1670 $z = 1.9433$
5086.27	0.79	0.971	0.165	5.885	
5134.07	0.33	0.823	0.119	6.916	
5320.27	1.15	0.644	0.160	4.025	Si II 1808 $z = 1.9433?$ S I 1803 $z = 1.9433?$
5455.91	0.87	0.630	0.159	3.962	Al III 1855 $z = 1.9433?$
5536.95	0.31	1.020	0.137	7.445	
5581.36	0.39	1.037	0.174	5.960	
6564.21	0.24	0.641	0.089	7.202	
6873.74	0.38	3.087	0.185	16.686	λ_{\oplus}
6897.79	0.32	5.329	0.211	25.256	Fe II 2344 $z = 1.9433$ λ_{\oplus}
6987.87	0.33	1.868	0.152	12.289	Fe II 2374 $z = 1.9433$
7011.50	0.25	5.304	0.194	27.340	Mg II 2796 $z = 1.5072$, Fe II 2383 $z = 1.9433$ (bl)
7028.62	0.70	0.836	0.146	5.726	Mg II 2803 $z = 1.5072$

Table 2—Continued

Central wavelength λ (Å, vacuum)	$\Delta\lambda^a$	Equivalent width W (Å)	ΔW	signif ^b	identification /comments ^{c,d}
7195.83	0.66	0.763	0.146	5.226	λ_{\oplus}
7606.77	0.18	16.070	0.291	55.223	λ_{\oplus}
7629.57	0.19	7.815	0.233	33.541	λ_{\oplus}
7653.95	0.37	11.034	0.334	33.036	Fe II 2600 $z = 1.9433$ λ_{\oplus}
8230.49	0.23	8.122	0.319	25.461	Mg II 2796 $z = 1.9433$ λ_{\oplus}
8251.27	0.33	7.438	0.351	21.191	Mg II 2803 $z = 1.9433$ λ_{\oplus}
8280.89	0.89	2.044	0.315	6.489	λ_{\oplus}
8323.14	1.23	1.900	0.338	5.621	
8355.79	0.66	1.578	0.258	6.116	
8394.65	0.70	1.347	0.234	5.756	Mg I 2852 $z = 1.9433$
8630.36	1.47	1.988	0.390	5.097	
8667.91	0.92	2.198	0.352	6.244	
9108.49	0.62	1.721	0.309	5.570	λ_{\oplus}
J104213+0619					
4668.71	0.70	1.524	0.265	5.751	
4787.50	0.78	0.747	0.144	5.188	
4798.76	0.73	0.742	0.135	5.496	
4818.97	0.81	1.745	0.244	7.152	
4866.27	0.83	1.189	0.131	9.076	
4916.56	1.15	0.906	0.140	6.471	
6282.88	0.97	1.143	0.148	7.723	
6874.80	0.26	3.085	0.152	20.296	λ_{\oplus}
6893.95	0.54	1.939	0.166	11.681	λ_{\oplus}
6907.41	0.50	0.815	0.118	6.907	λ_{\oplus}
6918.80	0.75	0.696	0.129	5.395	λ_{\oplus}
7198.82	0.90	2.474	0.194	12.753	λ_{\oplus}
7236.26	0.79	0.747	0.146	5.116	λ_{\oplus}
7607.89	0.20	15.031	0.279	53.875	λ_{\oplus}
7642.38	0.35	15.899	0.348	45.687	λ_{\oplus}
7723.50	1.08	1.199	0.225	5.329	
8233.02	0.83	2.116	0.307	6.893	λ_{\oplus}
8890.62	0.98	2.328	0.398	5.849	
8967.70	0.65	1.587	0.299	5.308	λ_{\oplus}
9058.41	0.79	1.684	0.330	5.103	

Table 2—Continued

Central wavelength λ (Å, vacuum)	$\Delta\lambda^a$	Equivalent width W (Å)	ΔW	signif ^b	identification /comments ^{c,d}
9105.85	0.99	2.711	0.422	6.424	λ_{\oplus}
J104323+0422					
4667.44	0.56	3.837	0.311	12.338	Fe II 2383 $z = 0.9585?$, CI 1657 $z = 1.8151?$, CIV 1548/1550 $z = 2.0121?$ (bl)
4705.27	0.38	4.293	0.286	15.010	Al II 1671 $z = 1.8151$
5033.88	0.49	2.271	0.239	9.502	Al II 1671 $z = 2.0121?$ (bl)
5092.36	1.17	0.565	0.191	2.958	Fe II 2600 $z = 0.9585$
5222.99	0.55	1.954	0.209	9.349	Al III 1855 $z = 1.8151$
5243.75	1.22	1.134	0.240	4.725	Al III 1863 $z = 1.8151$; Ni II 1742 $z = 2.0121?$ (bl)
5477.48	0.76	1.454	0.214	6.794	Mg II 2796 $z = 0.9585$
5490.31	0.59	0.963	0.164	5.872	Mg II 2803 $z = 0.9585$
5606.34	0.70	1.384	0.209	6.622	
6363.71	0.82	0.699	0.165	4.236	Fe II 2261 $z = 1.8151$
6419.84	1.30	1.084	0.204	5.314	
6600.02	0.27	3.835	0.198	19.369	Fe II 2344 $z = 1.8151$
6685.02	0.44	3.038	0.211	14.398	Fe II 2374 $z = 1.8151$
6708.32	0.19	4.978	0.187	26.620	Fe II 2383 $z = 1.8151$
6875.17	0.38	2.767	0.205	13.498	λ_{\oplus}
6893.81	1.15	1.078	0.214	5.037	λ_{\oplus}
7060.68	0.19	2.229	0.146	15.267	Fe II 2344 $z = 2.0121$
7153.05	0.79	1.143	0.196	5.832	Fe II 2374 $z = 2.0121$ (bl)
7176.85	0.23	4.925	0.198	24.874	Fe II 2383 $z = 2.0121$ (bl) λ_{\oplus}
7188.89	0.31	1.629	0.146	11.158	λ_{\oplus}
7202.35	0.46	2.488	0.197	12.629	λ_{\oplus}
7236.88	0.68	1.830	0.239	7.657	λ_{\oplus}
7255.71	0.48	1.588	0.190	8.358	Mn II 2577 $z = 1.8151$ λ_{\oplus}
7266.80	0.60	0.910	0.158	5.759	λ_{\oplus}
7282.02	0.35	5.376	0.297	18.101	Fe II 2587 $z = 1.8151$ λ_{\oplus}
7305.65	0.57	1.359	0.191	7.115	Mn II 2594 $z = 1.8151$ λ_{\oplus}
7320.58	0.26	5.736	0.259	22.147	Fe II 2600 $z = 1.8151$ λ_{\oplus}
7336.50	0.88	1.293	0.246	5.256	Mn II 2606 $z = 1.8151$ (bl)
7349.42	0.74	1.127	0.208	5.418	

Table 2—Continued

Central wavelength λ (Å, vacuum)	$\Delta\lambda^a$	Equivalent width W (Å)	ΔW	signif ^b	identification /comments ^{c,d}
7607.03	0.16	15.576	0.257	60.607	λ_{\oplus}
7632.53	0.16	9.512	0.223	42.655	λ_{\oplus}
7653.80	0.40	6.556	0.281	23.331	λ_{\oplus}
7790.19	0.43	2.251	0.239	9.418	Fe II 2587 $z = 2.0121$ (bl)
7829.39	0.10	9.348	0.208	44.942	Fe II 2600 $z = 2.0121$
7872.12	0.33	7.783	0.370	21.035	Mg II 2796 $z = 1.8151$
7893.07	0.20	7.206	0.274	26.299	Mg II 2803 $z = 1.8151$
8033.92	0.85	1.509	0.277	5.448	Mg I 2852 $z = 1.8151$
8164.45	1.38	1.571	0.290	5.417	λ_{\oplus}
8232.17	0.45	2.279	0.224	10.174	λ_{\oplus}
8279.64	1.15	2.152	0.392	5.490	λ_{\oplus}
8341.03	0.75	2.150	0.347	6.196	
8352.79	0.85	2.145	0.397	5.403	
8422.64	0.34	5.803	0.339	17.118	Mg II 2796 $z = 2.0121$
8445.00	0.38	5.825	0.320	18.203	Mg II 2803 $z = 2.0121$
8593.56	0.71	1.376	0.242	5.686	Mg I 2852 $z = 2.0121$
9135.55	0.58	1.546	0.259	5.969	λ_{\oplus}
9155.95	1.08	2.223	0.378	5.881	λ_{\oplus}
J104357+0438					
5024.69	0.80	0.797	0.158	5.044	Mg II 2796 $z = 0.7970$
5038.07	1.15	0.676	0.168	4.024	Mg II 2803 $z = 0.7970$
5238.75	0.71	0.275	0.085	3.235	Mg II 2796 $z = 0.8734$
5255.08	0.34	0.891	0.089	10.011	Mg II 2803 $z = 0.8734$ (bl)
5264.85	0.23	1.222	0.081	15.086	Mg II 2796 $z = 0.8828?$ + Fe II2600 $z = 1.0255$ (bl)
5292.51	0.34	0.626	0.074	8.459	
5301.70	0.65	0.469	0.088	5.330	
5664.06	0.41	1.385	0.125	11.080	Mg II 2796 $z = 1.0255$
5678.71	0.46	1.059	0.120	8.825	Mg II 2803 $z = 1.0255$
5777.71	1.08	0.915	0.157	5.828	Mg I 2852 $z = 1.0255$
5894.71	0.93	0.888	0.143	6.210	λ_{\oplus}
6297.34	0.76	0.731	0.138	5.297	
6874.70	0.27	3.923	0.168	23.351	λ_{\oplus}
6894.46	0.40	2.587	0.162	15.969	λ_{\oplus}

Table 2—Continued

Central wavelength λ (Å, vacuum)	$\Delta\lambda^a$	Equivalent width W (Å)	ΔW	signif ^b	identification /comments ^{c,d}
6909.81	0.44	0.898	0.114	7.877	λ_{\oplus}
6932.87	0.95	1.544	0.181	8.530	
6955.02	0.91	0.804	0.141	5.702	
7172.04	0.87	0.933	0.141	6.617	λ_{\oplus}
7187.80	0.42	1.946	0.143	13.608	Mg II 2796 $z = 1.5702$ (bl) λ_{\oplus}
7203.78	0.66	1.284	0.146	8.795	Mg II 2803 $z = 1.5702$ λ_{\oplus}
7248.06	0.94	0.960	0.157	6.115	λ_{\oplus}
7607.10	0.14	15.501	0.248	62.504	λ_{\oplus}
7634.09	0.17	11.365	0.238	47.752	λ_{\oplus}
7659.26	0.40	6.611	0.267	24.760	λ_{\oplus}
7697.25	0.81	1.469	0.208	7.062	
7830.18	0.39	0.333	0.113	2.947	Mg II 2796 $z = 1.8001?$
8166.43	0.78	0.942	0.181	5.204	λ_{\oplus}
8201.58	0.67	1.065	0.177	6.017	λ_{\oplus}
8230.63	0.77	1.384	0.206	6.718	λ_{\oplus}
8834.54	0.20	0.718	0.127	5.654	
J104409+0531					
4668.79	0.78	2.040	0.277	7.365	
4815.80	0.21	1.039	0.128	8.117	
4981.05	0.38	1.271	0.167	7.611	
5808.31	0.78	1.470	0.182	8.077	
5826.56	0.64	1.297	0.160	8.106	
5842.15	0.71	1.156	0.159	7.270	
5791.13	0.95	0.750	0.155	4.839	Mg II 2796 $z = 1.0710$
5808.31	0.78	1.470	0.182	8.077	Mg II 2803 $z = 1.0710$
6277.99	0.70	1.599	0.194	8.242	
6597.23	0.91	0.886	0.176	5.034	
6875.04	0.41	3.324	0.217	15.318	λ_{\oplus}
6889.63	0.57	0.674	0.134	5.030	λ_{\oplus}
6902.20	0.86	1.592	0.216	7.370	λ_{\oplus}
6963.35	0.71	0.961	0.169	5.686	
7027.06	0.63	0.868	0.158	5.494	
7176.63	0.62	0.833	0.149	5.591	λ_{\oplus}
7188.17	0.46	1.667	0.165	10.103	λ_{\oplus}

Table 2—Continued

Central wavelength λ (Å, vacuum)	$\Delta\lambda^a$	Equivalent width W (Å)	ΔW	signif ^b	identification /comments ^{c,d}
7198.49	0.37	0.983	0.124	7.927	λ_{\oplus}
7206.17	0.62	0.832	0.149	5.584	λ_{\oplus}
7413.59	0.77	0.926	0.178	5.202	
7563.14	0.76	0.934	0.175	5.337	
7607.26	0.17	16.141	0.243	66.424	λ_{\oplus}
7641.85	0.29	17.679	0.319	55.420	λ_{\oplus}
7679.28	0.47	0.816	0.133	6.135	λ_{\oplus}
7695.45	0.73	1.172	0.185	6.335	
8230.71	0.31	2.199	0.198	11.106	λ_{\oplus}
8991.03	0.66	1.785	0.294	6.071	λ_{\oplus}
9073.02	0.52	1.287	0.235	5.477	λ_{\oplus}
9134.65	0.51	1.317	0.235	5.604	λ_{\oplus}
9178.82	0.54	1.607	0.249	6.454	λ_{\oplus}
J104529+0623					
4764.66	1.21	1.525	0.291	5.241	
4819.66	0.24	6.105	0.180	33.917	
4842.84	0.24	1.353	0.095	14.242	
4851.02	0.37	0.872	0.094	9.277	
4875.50	0.51	4.063	0.212	19.165	
4895.32	0.80	0.951	0.189	5.032	
4956.87	0.96	1.310	0.274	4.781	Mg II 2796 $z = 0.7726$
4968.93	0.94	1.107	0.257	4.307	Mg II 2803 $z = 0.7726$
5144.16	0.64	0.959	0.178	5.388	
5153.51	0.56	1.075	0.173	6.214	
5555.66	0.60	1.107	0.192	5.766	
5576.94	0.49	2.631	0.278	9.464	
5585.46	0.42	0.818	0.148	5.527	
5807.68	0.70	1.019	0.177	5.757	Mg II 2796 $z = 1.0769$ (bl)
5822.67	1.20	0.583	0.173	3.370	Mg II 2803 $z = 1.0769$
5897.69	1.17	1.206	0.188	6.415	λ_{\oplus}
5926.09	1.01	0.573	0.126	4.548	Mg II 2796 $z = 1.1192$
5943.24	1.06	0.793	0.133	5.962	Mg II 2803 $z = 1.1192$
5967.20	0.13	0.414	0.046	9.000	
5993.73	1.41	0.801	0.151	5.305	

Table 2—Continued

Central wavelength λ (Å, vacuum)	$\Delta\lambda^a$	Equivalent width W (Å)	ΔW	signif ^b	identification /comments ^{c,d}
6874.56	0.31	4.350	0.233	18.670	λ_{\oplus}
6889.71	0.35	2.161	0.186	11.618	λ_{\oplus}
6902.10	0.56	1.995	0.215	9.279	λ_{\oplus}
6918.61	0.75	1.053	0.195	5.400	λ_{\oplus}
6950.85	0.77	1.021	0.196	5.209	
7514.30	1.23	2.145	0.326	6.580	Mg II 2796 $z = 1.6876$
7535.84	0.92	1.717	0.274	6.266	Mg II 2803 $z = 1.6876$
7608.03	0.18	16.702	0.342	48.836	λ_{\oplus}
7627.16	0.14	4.892	0.201	24.338	λ_{\oplus}
7648.34	0.40	14.046	0.424	33.127	λ_{\oplus}
7758.35	0.61	1.592	0.241	6.606	
7885.48	1.40	2.068	0.360	5.744	
7927.10	0.70	1.426	0.249	5.727	
8165.16	1.01	1.826	0.357	5.115	λ_{\oplus}
8231.78	0.82	1.923	0.341	5.639	λ_{\oplus}
8281.22	0.82	3.113	0.404	7.705	λ_{\oplus}
8346.12	0.56	3.598	0.388	9.273	
8459.58	0.68	1.695	0.334	5.075	
8766.22	0.67	4.400	0.339	12.979	
8839.01	0.45	4.599	0.398	11.555	
8890.24	0.74	4.739	0.505	9.384	
8925.27	0.89	3.650	0.515	7.087	
8956.31	0.75	2.353	0.436	5.397	
8966.35	0.77	2.396	0.460	5.209	λ_{\oplus}
J104543+0655					
5082.38	1.13	1.507	0.247	6.101	
5163.85	0.73	1.610	0.225	7.156	Fe II 2344 $z = 1.2028$ (bl)
5249.28	0.72	2.055	0.258	7.965	Fe II 2383 $z = 1.2028$
5333.13	0.33	3.327	0.240	13.863	Fe II 2344 $z = 1.2751$
5401.96	0.35	2.844	0.219	12.986	Fe II 2374 $z = 1.2751$
5421.10	0.53	4.886	0.298	16.396	Fe II 2383 $z = 1.2751$
5583.38	0.56	1.184	0.231	5.126	
5697.37	1.01	0.713	0.208	3.428	Fe II 2587 $z = 1.2028$
5727.68	0.50	2.171	0.235	9.238	Fe II 2600 $z = 1.2028$

Table 2—Continued

Central wavelength λ (Å, vacuum)	$\Delta\lambda^a$	Equivalent width W (Å)	ΔW	signif ^b	identification /comments ^{c,d}
5785.31	0.66	1.018	0.194	5.247	Fe II 2344 $z = 1.4684$
5860.84	0.64	1.160	0.183	6.339	Fe II 2374 $z = 1.4684$; Mn II 2577 $z = 1.2751$? (bl)
5883.41	0.26	5.521	0.228	24.215	Fe II 2587 $z = 1.2751$, Fe II2383 $z = 1.4684$ (bl)
5902.81	0.68	0.587	0.138	4.254	Mn II 2594 $z = 1.2751$? (bl λ_{\oplus})
5917.79	0.49	5.669	0.252	22.496	Fe II 2600 $z = 1.2751$ λ_{\oplus}
6159.68	0.31	3.822	0.231	16.545	Mg II 2796 $z = 1.2028$
6175.99	0.43	3.189	0.236	13.513	Mg II 2803 $z = 1.2028$
6282.55	1.41	2.343	0.318	7.368	Mg I 2852 $z = 1.2028$
6361.95	0.32	5.149	0.240	21.454	Mg II 2796 $z = 1.2751$
6380.18	0.30	6.016	0.240	25.067	Mg II 2803 $z = 1.2751$, Fe II2587 $z = 1.4684$ (bl)
6417.60	0.53	1.334	0.176	7.580	Fe II 2600 $z = 1.4684$
6490.56	0.50	1.943	0.188	10.335	Mg I 2852 $z = 1.2751$
6874.05	0.28	3.996	0.180	22.200	λ_{\oplus}
6888.16	0.28	1.174	0.114	10.298	λ_{\oplus}
6902.13	0.30	4.360	0.189	23.069	Mg II 2796 $z = 1.4684$ λ_{\oplus}
6920.69	0.40	2.065	0.161	12.826	Mg II 2803 $z = 1.4684$ λ_{\oplus}
6936.36	0.75	0.747	0.140	5.336	
6955.57	0.75	0.798	0.148	5.392	
7046.56	0.69	0.655	0.130	5.038	
7187.76	0.72	0.835	0.148	5.642	λ_{\oplus}
7202.23	1.04	1.558	0.216	7.213	λ_{\oplus}
7280.76	0.86	0.943	0.175	5.389	λ_{\oplus}
7294.88	0.90	1.247	0.194	6.428	λ_{\oplus}
7607.21	0.19	16.904	0.317	53.325	λ_{\oplus}
7628.28	0.13	5.778	0.191	30.251	λ_{\oplus}
7647.14	0.38	11.395	0.357	31.919	λ_{\oplus}
8231.14	0.73	1.577	0.283	5.572	λ_{\oplus}
8437.04	0.52	1.478	0.267	5.536	
8471.21	0.47	1.654	0.272	6.081	
8636.64	0.77	3.407	0.380	8.966	
8676.01	0.76	1.635	0.269	6.078	
8770.99	0.76	1.368	0.258	5.302	
8890.75	0.58	3.513	0.396	8.871	

Table 2—Continued

Central wavelength λ (Å, vacuum)	$\Delta\lambda^a$	Equivalent width W (Å)	ΔW	signif ^b	identification /comments ^{c,d}
9061.46	0.77	2.228	0.427	5.218	λ_{\oplus}
J104545+0523					
4866.14	0.71	2.519	0.311	8.100	
4961.75	1.09	1.869	0.320	5.841	
5176.46	0.65	1.975	0.248	7.964	Mg II 2796 $z = 0.8511$
5191.88	0.74	2.289	0.266	8.605	Mg II 2803 $z = 0.8511$
5274.32	0.84	1.042	0.216	4.824	Mg II 2796 $z = 0.8861$
5287.80	0.91	0.759	0.200	3.795	Mg II 2803 $z = 0.8861$
5581.56	0.67	0.925	0.178	5.197	
5899.43	1.01	0.984	0.192	5.125	λ_{\oplus}
6298.46	1.11	1.370	0.220	6.227	
6570.00	0.51	2.897	0.215	13.474	
6838.33	0.36	1.004	0.158	6.354	
6874.63	0.32	3.539	0.197	17.964	λ_{\oplus}
6894.57	0.60	1.552	0.181	8.575	λ_{\oplus}
6906.17	0.50	1.257	0.157	8.006	λ_{\oplus}
7166.05	1.05	1.091	0.200	5.455	λ_{\oplus}
7179.69	0.45	1.775	0.172	10.320	λ_{\oplus}
7193.51	0.48	1.672	0.174	9.609	λ_{\oplus}
7207.30	0.65	1.587	0.198	8.015	λ_{\oplus}
7237.67	0.92	1.934	0.238	8.126	λ_{\oplus}
7254.87	0.79	1.056	0.180	5.867	λ_{\oplus}
7293.65	0.90	1.325	0.208	6.370	λ_{\oplus}
7607.81	0.19	15.268	0.311	49.093	λ_{\oplus}
7628.77	0.18	5.352	0.211	25.365	λ_{\oplus}
7649.29	0.36	10.461	0.341	30.677	λ_{\oplus}
7676.35	0.57	1.415	0.199	7.111	λ_{\oplus}
8167.98	0.85	1.884	0.277	6.801	λ_{\oplus}
8232.50	1.53	3.131	0.416	7.526	λ_{\oplus}
8508.16	0.90	1.489	0.290	5.134	
8551.96	0.84	2.690	0.358	7.514	
8993.23	1.00	1.986	0.384	5.172	λ_{\oplus}
9008.03	0.92	1.774	0.353	5.025	λ_{\oplus}

Table 2—Continued

Central wavelength λ (Å, vacuum)	$\Delta\lambda^a$	Equivalent width W (Å)	ΔW	signif ^b	identification /comments ^{c,d}
J104552+0624					
4759.16	0.96	2.210	0.282	7.837	
5151.98	1.55	0.529	0.204	2.593	Ni II 2321 $z = 1.2199?$
5289.50	0.87	0.547	0.166	3.295	Fe II 2382 $z = 1.2199$
5772.02	1.25	0.458	0.165	2.776	Fe II 2600 $z = 1.2199?$
5990.02	0.36	2.239	0.176	12.722	
6207.89	0.34	1.786	0.149	11.987	Mg II 2796 $z = 1.2199$
6223.43	0.54	1.391	0.163	8.534	Mg II 2803 $z = 1.2199$
6752.64	0.66	1.767	0.184	9.603	
6768.51	0.40	0.620	0.109	5.688	
6875.22	0.25	3.825	0.166	23.042	λ_{\oplus}
6895.42	0.43	2.489	0.170	14.641	λ_{\oplus}
6914.26	0.57	1.920	0.172	11.163	λ_{\oplus}
6939.86	0.57	3.008	0.197	15.269	
6958.21	0.39	1.004	0.113	8.885	
6969.51	0.48	1.272	0.132	9.636	
6983.88	0.39	1.253	0.121	10.355	
6992.98	0.25	1.071	0.093	11.516	
7000.62	0.23	0.851	0.086	9.895	
7191.95	0.75	0.818	0.151	5.417	λ_{\oplus}
7207.39	1.10	0.950	0.182	5.220	λ_{\oplus}
7237.15	0.49	1.076	0.154	6.987	λ_{\oplus}
7607.31	0.13	15.604	0.214	72.916	λ_{\oplus}
7626.80	0.11	4.179	0.131	31.901	λ_{\oplus}
7644.01	0.17	10.867	0.220	49.395	λ_{\oplus}
7673.20	0.83	0.991	0.178	5.567	λ_{\oplus}
8167.64	0.63	1.694	0.205	8.263	λ_{\oplus}
8181.67	0.50	1.187	0.172	6.901	λ_{\oplus}
8199.07	0.49	0.982	0.168	5.845	λ_{\oplus}
8231.65	0.69	2.218	0.240	9.242	λ_{\oplus}
8967.82	0.46	1.927	0.258	7.469	λ_{\oplus}
8990.46	0.67	2.854	0.330	8.648	λ_{\oplus}
9020.38	1.16	1.986	0.332	5.982	λ_{\oplus}
9135.81	0.65	1.315	0.247	5.324	λ_{\oplus}

Table 2—Continued

Central wavelength λ (Å, vacuum)	$\Delta\lambda^a$	Equivalent width W (Å)	ΔW	signif ^b	identification /comments ^{c,d}
J104642+0531					
5094.18	0.54	6.341	0.347	18.274	
5127.33	0.76	4.432	0.345	12.846	
5533.61	0.89	1.789	0.253	7.071	
5545.86	0.75	1.811	0.235	7.706	
5654.47	0.19	11.734	0.268	43.784	Mg II 2796 $z = 1.0222$ (bl)
5669.19	0.12	14.172	0.236	60.051	Mg II 2803 $z = 1.0222$ (bl)
6264.19	1.00	0.959	0.184	5.212	
6280.21	0.89	1.226	0.189	6.487	
6312.88	1.09	1.457	0.249	5.851	
6875.25	0.27	3.469	0.165	21.024	λ_{\oplus}
6893.14	0.43	1.503	0.141	10.660	λ_{\oplus}
6905.82	0.66	0.994	0.142	7.000	λ_{\oplus}
7175.24	0.46	1.436	0.142	10.113	λ_{\oplus}
7187.60	0.27	1.889	0.125	15.112	λ_{\oplus}
7197.09	0.22	1.329	0.101	13.158	λ_{\oplus}
7207.00	0.32	1.954	0.135	14.474	λ_{\oplus}
7220.29	0.46	0.874	0.116	7.534	
7233.13	0.29	2.201	0.141	15.610	λ_{\oplus}
7245.81	0.32	2.583	0.180	14.350	λ_{\oplus}
7257.88	0.30	1.398	0.122	11.459	λ_{\oplus}
7266.95	0.29	1.034	0.105	9.848	λ_{\oplus}
7278.61	0.42	2.313	0.187	12.369	λ_{\oplus}
7293.34	0.39	1.450	0.139	10.432	λ_{\oplus}
7307.51	0.37	2.730	0.174	15.690	λ_{\oplus}
7322.88	0.50	1.533	0.165	9.291	λ_{\oplus}
7338.74	0.70	1.132	0.171	6.620	
7348.38	0.57	0.615	0.121	5.083	
7607.85	0.12	16.552	0.203	81.537	λ_{\oplus}
7639.88	0.19	16.054	0.242	66.339	λ_{\oplus}
7670.49	0.53	1.560	0.160	9.750	λ_{\oplus}
8030.08	0.82	1.813	0.234	7.748	
8160.99	0.62	3.908	0.245	15.951	λ_{\oplus}
8182.11	0.56	1.086	0.152	7.145	λ_{\oplus}
8193.80	0.50	0.971	0.141	6.887	λ_{\oplus}

Table 2—Continued

Central wavelength λ (Å, vacuum)	$\Delta\lambda^a$	Equivalent width W (Å)	ΔW	signif ^b	identification /comments ^{c,d}
8202.45	0.73	0.849	0.154	5.513	λ_{\oplus}
8234.59	0.54	4.590	0.251	18.287	λ_{\oplus}
8260.87	0.94	0.984	0.179	5.497	λ_{\oplus}
8281.87	0.73	2.809	0.274	10.252	λ_{\oplus}
8295.63	0.40	0.950	0.164	5.793	λ_{\oplus}
8323.67	1.24	2.199	0.279	7.882	
8355.92	0.87	2.164	0.297	7.286	
8436.14	0.67	1.716	0.249	6.892	
8469.09	1.02	1.503	0.266	5.650	
8727.60	1.00	1.618	0.235	6.885	
8770.87	0.58	2.941	0.331	8.885	
8893.45	0.67	1.919	0.281	6.829	
8945.11	0.87	1.292	0.244	5.295	
9137.34	0.90	1.505	0.236	6.377	λ_{\oplus}
9156.99	0.52	3.161	0.259	12.205	λ_{\oplus}
J104656+0541					
4790.03	1.28	1.075	0.340	3.162	Mg II 2796 $z = 0.7130$ (bl)
4803.63	1.04	1.316	0.338	3.893	Mg II 2803 $z = 0.7130$
5156.68	0.99	1.718	0.295	5.824	
5249.52	1.08	1.748	0.299	5.846	
6875.97	0.39	3.423	0.230	14.883	λ_{\oplus}
6892.73	0.48	1.899	0.198	9.591	λ_{\oplus}
6906.61	0.59	1.941	0.222	8.743	λ_{\oplus}
7188.73	0.58	2.119	0.214	9.902	λ_{\oplus}
7202.69	0.62	1.472	0.198	7.434	λ_{\oplus}
7607.33	0.16	13.907	0.262	53.080	λ_{\oplus}
7627.06	0.17	3.472	0.169	20.544	λ_{\oplus}
7644.42	0.29	10.134	0.299	33.893	λ_{\oplus}
7667.74	0.90	1.118	0.219	5.105	λ_{\oplus}
8160.04	0.54	1.018	0.191	5.330	λ_{\oplus}
8169.99	0.63	1.504	0.235	6.400	λ_{\oplus}
8180.86	0.71	1.350	0.238	5.672	λ_{\oplus}
8229.41	0.79	2.534	0.316	8.019	λ_{\oplus}
8970.08	1.11	3.258	0.525	6.206	λ_{\oplus}

Table 2—Continued

Central wavelength λ (Å, vacuum)	$\Delta\lambda^a$	Equivalent width W (Å)	ΔW	signif ^b	identification /comments ^{c,d}
8992.33	0.75	3.093	0.448	6.904	λ_{\oplus}
9087.42	0.78	1.776	0.343	5.178	λ_{\oplus}
J104733+0524					
5038.27	1.29	0.675	0.216	3.125	Mg II 2796 $z = 0.8016$
5050.45	1.17	0.739	0.215	3.437	Mg II 2803 $z = 0.8016$
5139.21	0.68	0.724	0.170	4.259	Mg I 2852 $z = 0.8016$
5205.02	0.21	4.992	0.231	21.610	
6395.08	0.35	2.574	0.172	14.965	
6632.33	0.57	0.601	0.119	5.050	
6874.62	0.58	3.457	0.233	14.837	λ_{\oplus}
6895.74	0.72	1.905	0.199	9.573	λ_{\oplus}
7173.25	0.59	1.914	0.195	9.815	λ_{\oplus}
7186.71	0.29	2.089	0.150	13.927	λ_{\oplus}
7202.28	0.60	2.731	0.220	12.414	λ_{\oplus}
7235.71	0.94	1.320	0.214	6.168	λ_{\oplus}
7247.21	0.65	0.997	0.188	5.303	λ_{\oplus}
7256.89	0.63	0.838	0.152	5.513	λ_{\oplus}
7607.48	0.13	15.184	0.220	69.018	λ_{\oplus}
7638.01	0.22	14.049	0.267	52.618	λ_{\oplus}
7665.63	0.54	1.896	0.196	9.673	λ_{\oplus}
8167.15	0.73	1.232	0.224	5.500	λ_{\oplus}
8182.57	0.65	1.361	0.220	6.186	λ_{\oplus}
8199.28	0.94	1.425	0.258	5.523	λ_{\oplus}
8232.18	0.72	1.891	0.262	7.218	λ_{\oplus}
J104747+0456					
4533.44	0.87	3.398	0.510	6.663	
4642.00	0.57	1.337	0.220	6.077	
4658.96	0.53	1.147	0.211	5.436	
4684.25	0.58	3.050	0.306	9.967	
4735.33	0.39	5.933	0.286	20.745	Mg II 2796 $z = 0.6950$ (bl); CIV 1548/1550 $z = 2.0728?$
4754.13	0.27	6.015	0.233	25.815	Mg II 2803 $z = 0.6950$ (bl)

Table 2—Continued

Central wavelength λ (Å, vacuum)	$\Delta\lambda^a$	Equivalent width W (Å)	ΔW	signif ^b	identification /comments ^{c,d}
4859.17	1.00	1.076	0.186	5.785	
4936.36	0.79	0.809	0.185	4.373	Mg II 2796 $z = 0.7653$
4949.75	1.16	0.426	0.171	2.491	Mg II 2803 $z = 0.7653$
4984.92	0.91	2.540	0.288	8.819	
5130.69	0.38	3.462	0.206	16.806	Mg II 2796 $z = 0.8341$ (bl)
5144.62	0.61	0.437	0.116	3.767	Mg II 2803 $z = 0.8341$
5153.16	0.59	0.883	0.150	5.887	
6281.25	0.97	1.339	0.225	5.951	Mg II 2796 $z = 1.2455?$
6291.79	0.78	0.404	0.137	2.949	Mg II 2803 $z = 1.2455?$ (heavily bl)
6320.74	0.78	1.811	0.244	7.422	
6876.97	0.54	3.321	0.259	12.822	λ_{\oplus}
6893.35	0.50	1.393	0.173	8.052	λ_{\oplus}
6902.53	0.38	1.053	0.138	7.630	λ_{\oplus}
7175.90	0.29	2.729	0.174	15.684	λ_{\oplus}
7190.56	0.47	1.311	0.152	8.625	λ_{\oplus}
7204.08	0.32	3.274	0.185	17.697	Fe II 2344 $z = 2.0728$ (bl λ_{\oplus})
7296.57	0.55	1.166	0.187	6.235	Fe II 2374 $z = 2.0728$ λ_{\oplus}
7309.50	0.55	0.848	0.163	5.202	λ_{\oplus}
7321.43	0.28	4.032	0.242	16.661	Fe II 2383 $z = 2.0728$ λ_{\oplus}
7611.03	0.12	15.204	0.214	71.047	λ_{\oplus}
7634.38	0.14	7.774	0.188	41.351	λ_{\oplus}
7650.83	0.17	6.008	0.174	34.529	λ_{\oplus}
7665.46	0.33	2.098	0.171	12.269	λ_{\oplus}
7680.90	0.73	1.536	0.195	7.877	λ_{\oplus}
7832.62	0.12	8.095	0.206	39.296	
7947.92	0.75	2.148	0.278	7.727	Fe II 2587 $z = 2.0728$
7989.57	0.37	3.409	0.273	12.487	Fe II 2600 $z = 2.0728$
8196.96	0.52	2.682	0.240	11.175	Mg II 2796 $z = 1.9312$ (bl) λ_{\oplus}
8216.89	0.75	0.670	0.174	3.851	Mg II 2803 $z = 1.9312$ λ_{\oplus}
8234.38	0.47	2.468	0.222	11.117	λ_{\oplus}
8592.36	0.16	7.253	0.218	33.271	Mg II 2796 $z = 2.0728$
8614.91	0.41	7.370	0.350	21.057	Mg II 2803 $z = 2.0728$
8765.76	0.74	0.724	0.231	3.134	Mg I 2852 $z = 2.0728$
8847.89	1.10	2.269	0.431	5.265	

Table 2—Continued

Central wavelength λ (Å, vacuum)	$\Delta\lambda^a$	Equivalent width W (Å)	ΔW	signif ^b	identification /comments ^{c,d}
5893.08	0.65	0.835	0.158	5.285	λ_{\oplus}
6128.07	0.91	1.163	0.205	5.673	
6874.24	0.40	3.677	0.231	15.918	λ_{\oplus}
6892.90	0.80	1.586	0.220	7.209	λ_{\oplus}
7173.35	0.87	1.123	0.213	5.272	λ_{\oplus}
7186.40	0.46	2.056	0.207	9.932	λ_{\oplus}
7198.32	0.59	1.035	0.176	5.881	λ_{\oplus}
7278.25	0.65	0.960	0.181	5.304	λ_{\oplus}
7607.88	0.22	15.608	0.378	41.291	λ_{\oplus}
7641.82	0.45	16.234	0.486	33.403	λ_{\oplus}
8165.17	0.94	1.929	0.348	5.543	λ_{\oplus}
8230.33	1.03	2.758	0.412	6.694	λ_{\oplus}
8474.91	0.37	1.618	0.260	6.223	
J104840+0535					
4654.73	1.96	2.861	0.442	6.473	
4738.41	0.85	1.386	0.255	5.435	Fe II 2383 $z = 0.9882$ (bl)?
5142.25	0.81	1.687	0.217	7.774	Fe II 2586 $z = 0.9882$ (bl)?
5169.18	0.50	1.345	0.167	8.054	Fe II 2600 $z = 0.9882$
5559.66	0.26	2.222	0.142	15.648	Mg II 2796 $z = 0.9882$
5573.81	0.19	3.003	0.142	21.148	Mg II 2803 $z = 0.9882$
5894.22	0.94	1.061	0.192	5.526	λ_{\oplus}
5911.38	1.08	0.515	0.160	3.219	Fe II 2600 $z = 1.2728?$ λ_{\oplus}
6282.77	0.86	0.715	0.151	4.735	Mg II 2796 $z = 1.2460$ (bl)
6296.83	0.77	0.929	0.178	5.219	Mg II 2803 $z = 1.2460$
6309.78	0.56	1.323	0.161	8.217	
6335.09	0.72	2.647	0.221	11.977	
6356.18	0.41	1.175	0.141	8.333	Mg II 2796 $z = 1.2728$ (bl)
6371.43	0.59	0.450	0.115	3.913	Mg II 2803 $z = 1.2728$
6877.07	0.25	4.052	0.163	24.859	λ_{\oplus}
6893.53	0.37	1.046	0.113	9.257	λ_{\oplus}
6902.96	0.49	0.599	0.102	5.873	λ_{\oplus}
6910.65	0.58	0.681	0.115	5.922	λ_{\oplus}
7172.91	0.91	0.787	0.155	5.077	λ_{\oplus}

Table 2—Continued

Central wavelength λ (Å, vacuum)	$\Delta\lambda^a$	Equivalent width W (Å)	ΔW	signif ^b	identification /comments ^{c,d}
7182.17	0.41	0.793	0.114	6.956	λ_{\oplus}
7189.64	0.48	0.679	0.114	5.956	λ_{\oplus}
7608.87	0.17	16.527	0.307	53.834	λ_{\oplus}
7644.16	0.37	18.692	0.418	44.718	λ_{\oplus}
7737.45	1.01	1.661	0.325	5.111	
8202.76	0.78	1.005	0.193	5.207	λ_{\oplus}
8232.72	0.69	1.563	0.208	7.514	λ_{\oplus}
8969.82	0.89	1.769	0.340	5.203	λ_{\oplus}
J104914+0414					
5038.32	0.87	1.357	0.187	7.257	
6278.62	1.28	0.962	0.194	4.959	Mg II 2796 $z = 1.2458$
6297.95	0.59	1.256	0.161	7.801	Mg II 2803 $z = 1.2458$ (bl)
6308.84	0.27	0.635	0.100	6.350	
6781.62	0.57	0.290	0.096	3.021	Mg II 2796 $z = 1.4252?$
6813.82	0.42	0.859	0.124	6.927	
6875.28	0.34	2.983	0.174	17.144	λ_{\oplus}
6890.69	0.41	1.058	0.127	8.331	λ_{\oplus}
6897.27	0.32	0.430	0.080	5.375	λ_{\oplus}
6906.98	0.44	1.893	0.161	11.758	λ_{\oplus}
6921.90	0.61	1.145	0.152	7.533	λ_{\oplus}
7178.34	1.10	1.334	0.231	5.775	λ_{\oplus}
7193.41	0.55	1.352	0.161	8.398	λ_{\oplus}
7205.45	0.61	0.817	0.145	5.634	λ_{\oplus}
7254.07	1.55	1.395	0.234	5.962	λ_{\oplus}
7607.73	0.23	15.309	0.357	42.882	λ_{\oplus}
7626.83	0.18	3.875	0.201	19.279	λ_{\oplus}
7644.00	0.34	10.416	0.362	28.773	λ_{\oplus}
8231.04	1.17	1.603	0.296	5.416	λ_{\oplus}
8970.47	0.65	3.215	0.401	8.017	λ_{\oplus}
J104929+0544					
5037.35	0.76	1.338	0.221	6.054	
5049.36	0.40	1.588	0.182	8.725	

Table 2—Continued

Central wavelength λ (Å, vacuum)	$\Delta\lambda^a$	Equivalent width W (Å)	ΔW	signif ^b	identification /comments ^{c,d}
5060.29	0.25	3.136	0.194	16.165	
5074.03	0.22	5.936	0.229	25.921	
5098.05	0.38	8.034	0.309	26.000	
5121.74	0.50	1.908	0.208	9.173	
5134.30	0.67	0.970	0.187	5.187	
5788.65	1.74	0.902	0.247	3.652	Fe II 2600 $z = 1.2264$
6214.01	0.35	0.958	0.146	6.562	
6226.14	0.85	1.359	0.224	6.067	Mg II 2796 $z = 1.2264$
6240.95	0.74	0.951	0.203	4.685	Mg II 2803 $z = 1.2264$
6552.28	0.65	1.492	0.210	7.105	
6634.44	0.80	1.088	0.189	5.757	
6658.92	0.38	2.314	0.188	12.309	
6836.05	0.45	3.044	0.239	12.736	
6873.58	0.69	4.045	0.286	14.143	λ_{\oplus}
6895.23	0.50	2.009	0.192	10.464	λ_{\oplus}
6909.76	0.40	2.500	0.194	12.887	λ_{\oplus}
6924.25	0.62	1.174	0.181	6.486	
7175.92	0.64	1.267	0.177	7.158	λ_{\oplus}
7189.99	0.37	2.580	0.183	14.098	λ_{\oplus}
7204.87	0.51	1.940	0.192	10.104	λ_{\oplus}
7227.88	0.61	1.988	0.209	9.512	Mg II 2796 $z = 1.5851$
7248.90	0.76	1.815	0.267	6.798	Mg II 2803 $z = 1.5851$ λ_{\oplus}
7266.26	0.34	2.991	0.198	15.106	λ_{\oplus}
7279.42	0.88	1.370	0.261	5.249	λ_{\oplus}
7608.27	0.14	15.088	0.244	61.836	λ_{\oplus}
7632.30	0.13	9.167	0.203	45.158	λ_{\oplus}
7655.15	0.29	12.435	0.309	40.243	λ_{\oplus}
7814.49	0.19	4.248	0.196	21.673	
7830.08	0.09	10.544	0.178	59.236	
8138.74	0.80	1.014	0.201	5.045	λ_{\oplus}
8162.68	0.73	4.246	0.316	13.437	λ_{\oplus}
8186.05	0.44	2.709	0.228	11.882	λ_{\oplus}
8198.79	0.74	1.141	0.210	5.433	λ_{\oplus}
8231.03	0.72	2.606	0.273	9.546	λ_{\oplus}
8306.98	0.15	2.166	0.188	11.521	λ_{\oplus}
9165.46	0.52	1.520	0.274	5.547	λ_{\oplus}

Table 2—Continued

Central wavelength λ (Å, vacuum)	$\Delta\lambda^a$	Equivalent width W (Å)	ΔW	signif ^b	identification /comments ^{c,d}
J105010+0432					
6874.24	0.39	3.903	0.222	17.581	λ_{\oplus}
6888.89	0.40	0.927	0.128	7.242	λ_{\oplus}
6902.39	0.80	2.322	0.231	10.052	λ_{\oplus}
7176.59	0.75	1.651	0.195	8.467	λ_{\oplus}
7190.13	0.43	1.713	0.159	10.774	λ_{\oplus}
7204.80	0.43	1.774	0.166	10.687	λ_{\oplus}
7239.59	1.11	1.981	0.272	7.283	λ_{\oplus}
7608.35	0.12	14.992	0.209	71.732	λ_{\oplus}
7643.35	0.35	15.987	0.331	48.299	λ_{\oplus}
8146.60	1.48	1.923	0.308	6.244	λ_{\oplus}
8167.29	0.70	1.907	0.232	8.220	λ_{\oplus}
8232.17	0.60	2.400	0.252	9.524	λ_{\oplus}
8991.66	0.73	2.153	0.390	5.521	λ_{\oplus}

^a 1σ uncertainty in feature centroid

^bsignificance ($W/\Delta W$)

^cbl = blend

^d λ_{\oplus} = in telluric absorption zone

Table 3. Mg II systems

quasar	z_{MgII}^a	type ^b	survey		cl ^e	$W_0(\lambda 2796)$ (Å)	$\sigma(\lambda 2796)$	$W_0(\lambda 2803)$ (Å)	$\sigma(\lambda 2803)$	comments /other metals
			s ^c	w ^d						
J103937+0531	1.1448	w	n	y	r	0.342 ± 0.102	3.362	0.220 ± 0.083	2.661	
J103937+0531	1.2515	w	n	n	c	0.494 ± 0.101	4.877	0.202 ± 0.074	2.725	
J103937+0531	1.9748	w	n	y	r	0.436 ± 0.113	3.872	0.374 ± 0.083	4.492	
J103952+0633	1.2459	w	n	y	r	0.329 ± 0.077	4.272	0.678 ± 0.081	8.409	Fe II $W_{0,2600} = 0.246$
J103952+0633	1.3353	w	n	y	r	0.339 ± 0.085	4.000	0.311 ± 0.075	4.172	
J104007+0531	1.3015	w	n	y	r	0.566 ± 0.068	8.293	0.426 ± 0.056	7.656	Mg I?; Fe II $W_{0,2600} = 0.295$
J104007+0531	1.5706 ^f	s	y	y	r	3.462 ± 0.115	30.061	2.846 ± 0.101	28.142	Fe II $W_{0,2600} = 1.305$
J104155+0612	0.8829	s	y	y	r	0.933 ± 0.092	10.092	1.034 ± 0.088	11.794	
J104155+0612	0.9376	s	y	y	r	0.714 ± 0.071	10.029	0.631 ± 0.078	8.093	Fe II, Mg I
J104155+0612	1.2628	w	n	y	r	0.375 ± 0.051	7.383	0.320 ± 0.054	5.894	
J104155+0612	1.3460	w	n	y	r	0.316 ± 0.054	5.889	0.238 ± 0.050	4.737	
J104213+0628	1.5072	s	y	y	r	2.115 ± 0.077	27.340	0.333 ± 0.058	5.726	
J104213+0628	1.9433 ^f	s	y	y	r	2.759 ± 0.108	25.461	2.527 ± 0.119	21.191	Fe II $W_{0,2600} = 3.748$, Mg I, Al II; Si II?, S I?, Al III?
J104323+0422	0.9585	s	y	y	r	0.742 ± 0.109	6.794	0.492 ± 0.084	5.872	Fe II $W_{0,2600} = 0.288?$
J104323+0422	1.8151 ^f	s	y	y	r	2.765 ± 0.131	21.035	2.559 ± 0.097	26.299	C I?, Al II, Al III, Mn II, Mg I, Fe II $W_{0,2600} = 2.037$
J104323+0422	2.0121 ^f	s	y	y	r	1.927 ± 0.113	17.118	1.934 ± 0.106	18.203	C IV?, Mg I, Al II?; Fe II $W_{0,2600} = 3.105$
J104357+0438	0.7970	w	n	y	r	0.444 ± 0.088	5.044	0.376 ± 0.093	4.024	

Table 3. Mg II systems (continued)

quasar	z_{MgII}^a	type ^b	survey		cl ^e	$W_0(\lambda 2796)$ (Å)	$\sigma(\lambda 2796)$	$W_0(\lambda 2803)$ (Å)	$\sigma(\lambda 2803)$	comments /other metals
			s ^c	w ^d						
J104357+0438	0.8734	v	n	n	c	0.147 ± 0.045	3.235	0.476 ± 0.048	10.011	
J104357+0438	1.0255 ^f	s	y	y	r	0.684 ± 0.062	11.080	0.523 ± 0.059	8.825	Mg I, Fe II (bl) $W_{0,2600} = 0.604$
J104357+0438	1.5702	s	y	y	r	0.757 ± 0.056	13.608	0.500 ± 0.057	8.795	
J104409+0531	1.0710	w	n	y	r	0.362 ± 0.075	4.839	0.710 ± 0.088	8.077	
J104529+0623	0.7726	s	y	y	r	0.739 ± 0.155	4.781	0.625 ± 0.145	4.307	
J104529+0623	1.0769	w	n	y	r	0.491 ± 0.085	5.757	0.281 ± 0.083	3.370	
J104529+0623	1.1192	v	n	n	d	0.270 ± 0.059	4.548	0.374 ± 0.063	5.962	
J104529+0623	1.6876	s	y	y	r	0.798 ± 0.121	6.580	0.639 ± 0.102	6.266	
J104543+0655	1.2028 ^f	s	y	y	r	1.735 ± 0.105	16.545	1.448 ± 0.107	13.513	Fe II $W_{0,2600} = 0.986$, Mg I
J104543+0655	1.2751 ^f	s	y	y	r	2.263 ± 0.105	21.454	2.643 ± 0.105	25.067	Mn II?; Mg I, Fe II $W_{0,2600} = 2.491$
J104543+0655	1.4684 ^f	s	y	y	r	1.766 ± 0.077	23.069	0.837 ± 0.065	12.826	Fe II $W_{0,2600} = 0.540$
J104545+0523	0.8511	s	y	y	r	1.067 ± 0.134	7.964	1.236 ± 0.144	8.605	
J104545+0523	0.8861	w	n	y	r	0.552 ± 0.115	4.824	0.402 ± 0.106	3.795	profile blended
J104552+0624	1.2199	s	y	y	r	0.805 ± 0.067	11.987	0.627 ± 0.073	8.534	Ni II?; Fe II $W_{0,2600} = 0.206$
J104642+0531	1.0222	s	y	y	r	5.803 ± 0.133	43.784	7.008 ± 0.117	60.051	
J104656+0541	0.7130	s	y	n	r	0.628 ± 0.198	3.162	0.768 ± 0.197	3.893	
J104733+0524	0.8016	w	n	y	r	0.375 ± 0.120	3.125	0.410 ± 0.119	3.437	Mg I
J104747+0456	0.6950	s	y	y	r	3.500 ± 0.169	20.745	3.549 ± 0.137	25.815	
J104747+0456	0.7653	w	n	n	c	0.458 ± 0.105	4.373	0.241 ± 0.097	2.491	

Table 3. Mg II systems (continued)

quasar	z_{MgII}^a	type ^b	survey		cl ^e	$W_0(\lambda 2796)$ (Å)	$\sigma(\lambda 2796)$	$W_0(\lambda 2803)$ (Å)	$\sigma(\lambda 2803)$	comments /other metals
			s ^c	w ^d						
J104747+0456	0.8341	s	y	y	r	1.887 ± 0.112	16.806	0.238 ± 0.063	3.767	
J104747+0456	1.2455	w	n	n	c	0.596 ± 0.100	5.951	0.180 ± 0.061	2.949	
J104747+0456	1.9312	s	y	y	r	0.915 ± 0.082	11.175	0.229 ± 0.059	3.851	
J104747+0456	2.0728 ^f	s	a	a	r	2.360 ± 0.071	33.271	2.398 ± 0.114	21.057	Fe II $W_{0,2600} = 1.109$, Mg I; C IV?
J104840+0535	0.9882 ^f	s	y	y	r	1.118 ± 0.071	15.648	1.510 ± 0.071	21.148	Fe II $W_{0,2600} = 0.677$
J104840+0535	1.2460	w	n	n	c	0.318 ± 0.067	4.735	0.414 ± 0.079	5.219	
J104840+0535	1.2728	w	n	y	r	0.517 ± 0.062	8.333	0.198 ± 0.051	3.913	Fe II $W_{0,2600} = 0.227?$
J104914+0414	1.2458	w	n	y	r	0.428 ± 0.086	4.959	0.559 ± 0.072	7.801	
J104914+0414	1.4252	v	n	n	r	0.120 ± 0.040	3.021	0.610 ± 0.101	6.067	
J104929+0544	1.2264 ^f	s	y	y	r	0.427 ± 0.091	4.685	0.769 ± 0.081	9.512	Fe II $W_{0,2600} = 1.2263$
J104929+0544	1.5851	s	y	y	r	0.702 ± 0.103	6.798	0.342 ± 0.102	3.362	

^aredshift is determined by centroid of both Mg II components, with an attempt to correct for blending.

^bs: strong ($W_{0,\lambda 2796} \geq 0.6 \text{ \AA}$); w: weak ($0.3 \leq W_0 < 0.6 \text{ \AA}$); v: very weak ($W_0 < 0.3 \text{ \AA}$)

^cy: in strong survey; n: not in strong survey; a: associated system (excluded)

^dy: in weak survey; n: not in weak survey; a: associated system (excluded)

^eclass: r: real; c: candidate; d: doubtful

^fcandidate damped system ($W_{0,MgII\ 2796} \geq 0.5 \text{ \AA}$ and $W_{0,FeII\ 2600} \geq 0.5 \text{ \AA}$)

Table 4. Mg II sample

sample	total path Δz	observed Mg II	expected Mg II
Weak: $W_0(\lambda 2796) \geq 0.3 \text{ \AA}$	24.13	38	24.0
Strong: $W_0(\lambda 2796) \geq 0.6 \text{ \AA}$	25.75	26	14.0

Table 5. Quasar-Mg II pairs with $-4500 < \Delta v < -3000 \text{ km s}^{-1}$ and $\Delta \ell < 9h^{-1} \text{ Mpc}$

quasar	z_Q	Mg II toward quasar	z_{MgII}	Δv^a	$\Delta \ell^b$ ($h^{-1} \text{ Mpc}$)	class (strong/weak)
J103908+0459	1.942	J103936+0531	1.9748	-3330	8.1	w
J104117+0610	1.273	J104007+0531	1.3015	-3740	5.9	w
J104149+0643	1.316	J104155+0612	1.3460	-3860	8.0	w
J104155+0612	1.480	J104213+0628	1.5072	-3270	4.3	s
J104200+0441	1.97	J104323+0422	2.0121	-4220	7.0	s
J104336+0558 ^c	1.236	J104155+0612	1.2628	-3570	7.4	w
J105010+0432	1.217	J104914+0414	1.2458	-3870	5.9	w
J105030+0430	1.215	J104914+0414	1.2458	-4140	6.4	w

^a $\Delta v \equiv c(z_Q - z_{MgII}) / (0.5(2 + z_Q + z_{MgII}))$

^bprojected distance in the plane of the sky

^cposition not in Veron-Cetty & Veron (2001); RA=10:43:36.6, dec=05:58:48 (J2000)

This figure "f1a.jpeg" is available in "jpeg" format from:

<http://arxiv.org/ps/astro-ph/0111135v2>

This figure "f1b.jpeg" is available in "jpeg" format from:

<http://arxiv.org/ps/astro-ph/0111135v2>

This figure "f1c.jpeg" is available in "jpeg" format from:

<http://arxiv.org/ps/astro-ph/0111135v2>

This figure "f1d.jpeg" is available in "jpeg" format from:

<http://arxiv.org/ps/astro-ph/0111135v2>

This figure "f1e.jpeg" is available in "jpeg" format from:

<http://arxiv.org/ps/astro-ph/0111135v2>

This figure "f1f.jpeg" is available in "jpeg" format from:

<http://arxiv.org/ps/astro-ph/0111135v2>